SJIE 1(1) X–X (2025) https://doi.org/XXXX/XXXX

Zinc-Copper Galvanic Half-Cells: LED Powering and Real-World Potential

Dinara Kalupahana, Matyas Vyhnalek, Minh Tri Truong, Rakeisha Heidi Liem, Shael Caden Chandran, Jordan Kambanis, Masoomeh Asgharnejad-laskoukalayeh, Benedict Tai,
David Alam, Thomas Whittle, Yi Shen, Gobinath Rajarathnam
School of Chemical and Biomolecular Engineering, Faculty of Engineering, The University of Sydney, New South Wales, Australia

Abstract

This experiment investigated the production and performance of zinc-copper galvanic cells using accessible materials, with a focus on optimizing voltage output and understanding factors influencing cell efficiency. By varying the factors such as electrolyte concentration, electrode materials, and cell configuration (single cells vs. series connection), we analysed their impact on voltage, current, and ability to power LEDs of varying voltage thresholds. Three electrolyte concentrations (0.1M, 0.5M, 1M, 2M) were tested in different combinations for both zinc sulfate and copper(II) sulfate solutions. Results showed minimal variation in voltage with changing concentration alone, with values ranging from approximately 0.9996 V to 1.0293 V. However, connecting multiple cells in series significantly increased voltage, with three cells in series reaching a voltage of 3.0656 V, which was sufficient to power all tested LED colors. These findings combined with theoretical predictions of Zn-Cu cells, demonstrated fundamental electrochemical principles such as redox reactions and ion migration via salt bridges. The experiment highlights the scalability and practical relevance of galvanic cells for real-world energy applications, reinforcing their role in the ongoing pursuit of efficient, low-cost, and sustainable battery technologies.

1. Introduction

The escalating demand for portable and sustainable energy solutions has catalysed advancements in electrochemical systems, notably galvanic (voltaic) cells, which facilitate the conversion of chemical energy into electrical energy through spontaneous redox reactions.[1] In galvanic cells, oxidation and reduction processes occur at separate electrodes, generating a flow of electrons through an external circuit which produces an electrical current. This fundamental principle underpins the operation of various battery types, including primary cells such as zinc-carbon batteries and secondary cells like lithium-ion batteries.[2]

A galvanic cell comprises two half-cells, each containing an electrode immersed in an electrolyte

SJIE 1(1) X–X (2025) https://doi.org/XXXX/XXXX

solution, which are connected by a salt bridge or porous membrane. In this electrochemical system, oxidation occurs at the anode - where metal atoms lose electrons to form cations - which then enter the electrolyte solution. The free electrons flow through an external circuit to the cathode, where reduction takes place - cations in the electrolyte gain electrons and are reduced to neutral atoms.[1] The salt bridge preserves the electrical neutrality of the galvanic cell by facilitating the migration of ions between the half-cells, thereby completing the circuit and sustaining the continuous flow of electrons necessary to generate an electrical current.[3]

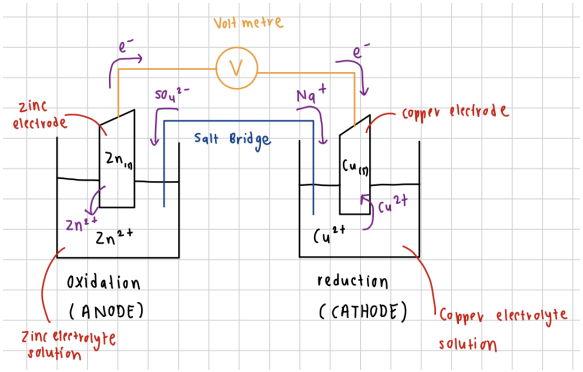

Image 1: Diagram of Zn/Cu half cells with indicated species flows shown

A comprehensive understanding of such principles is fundamental in the field of electrochemical engineering, particularly in the design and optimisation of battery technologies.[4] For instance, the performance characteristics of a battery - voltage, capacity, and efficiency - are influenced by various factors, including the selection of electrode materials, the composition of the electrolyte, and the internal resistance of the cell.[5] By systematically applying this foundational knowledge, engineers can produce energy storage systems that are optimized for safety, longevity, and environmental sustainability, further aligning with the specific demands of the diverse applications of such batteries, including electric vehicles and future developments of sustainable energy solutions.[6]

2. Materials and Methods

2.1: Materials

Copper foil (electrode)	Zinc foil (electrode)
Cotton rope and plastic salt-bridge spacer	Centrifuge tubes
2M Copper(II) sulfate ($CuSO_4$) solution	Centrifuge tube holder
2M Zinc sulfate ($ZnSO_4$) solution	Multimeter
2M Potassium chloride (KCl) solution	5 LED lights (green, blue, white, yellow, red)
Wires	Alligator Clips
Scissors	3 AA Batteries

2.2: Experimental Method

2.2.1: Preparation of materials and solutions

Copper and zinc foils were prepared by cutting out four 3 cm × 6 cm strips of each electrode species. 10mL of the 2M potassium chloride (KCl) solution was added to a 500mL beaker, along with 190mL of water, to produce a 0.1M KCL solution. The other electrolyte solutions (copper (II) sulfate ($CuSO_4$) and zinc sulfate ($ZnSO_4$)) were prepared in separate 500mL beakers at four different concentrations: 0.1M, 0.5M, 1M and 2M:

0.1M solution: 10mL of 2M base solution and 190mL of water added to a 500mL beaker 0.5M solution: 50mL of 2M base solution and 150 mL of water added to a 500mL beaker 1M solution: 100mL of 2M base solution and 100mL of water added to a 500mL beaker 2M solution: 200mL of 2M base solution added to a 500mL beaker.

A strip of cotton rope was placed in the 0.1M KCl solution, allowing the material to soak up the solution. The strip of cotton rope was then placed

into the plastic salt-bridge spacer. Five LEDs of varying colours (and thus varying voltages required) were collected and tested in increasing voltage requirements (red → green) using one or more AA batteries to determine which terminal was negative and positive.

2.2.2: Testing varying electrolyte concentrations in galvanic half-cells

Four galvanic half-cells were made using varying electrolyte concentrations (0.1M, 0.5M, 1M, and 2M). For each galvanic half-cell, one centrifuge tube filled approximately two thirds full with $CuSO_4$, and second approximately two thirds full with $ZnSO_4$. Both electrolyte solutions would be of the same concentration. A strip of copper foil was placed in the copper (II) sulfate centrifuge tube, and a strip of zinc foil was placed in the zinc sulfate centrifuge tube. The salt bridge (cotton rope in plastic spacer) was placed in the two centrifuge tubes to connect the solutions. See *Figure 1* below for an image of a prepared galvanic half-cell.Wires were then attached to the electrode foils using crocodile clips.

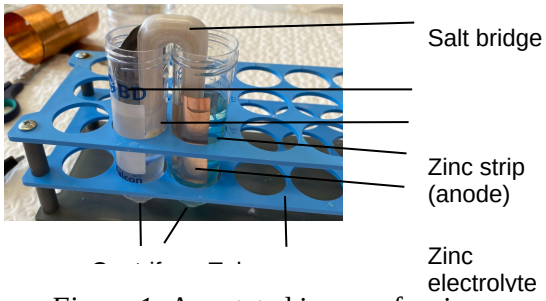

Figure 1: Annotated image of a zinc-copper galvanic half-cell

The wire from the copper electrode was connected to the positive terminal of the multimeter, and the wire from the zinc electrode was connected to the negative terminal of the multimeter. Voltage readings were taken for each of the electrolyte concentrations. The wires from each galvanic half-cell were then disconnected from the multimeter and connected to the appropriate terminals on the green LED to determine whether the voltage was high enough to power it or not.

2.2.3: Testing several galvanic half-cells in Series

Following the voltage and current readings using individual galvanic half-cells, the galvanic half-cells were connected in series. This was achieved using wires with alligator clips connecting the anode (zinc foil) to the cathode (copper foil). First, only two galvanic half-cells (0.1M and 1M concentrations) were connected in series, and voltage readings were taken using the multimeter. Then, three galvanic half-cells (0.1M, 1M and 2M concentrations) were connected in series, and voltage readings were taken using the multimeter. The wires were then disconnected from the multimeter and connected to the appropriate terminals on the LEDs to determine whether each colour could be turned on or not, starting with green (highest voltage requirement), and then blue, white, yellow and finally red (lowest voltage requirement.

2.2.4: Analysis Techniques

Several forms of raw data were collected and analysed during this process. A multimeter was used to measure voltage and current of the various individual galvanic half-cells, as well as that of several galvanic half-cells in series. Additionally, LEDs of different colours were used to test the performance of multiple galvanic half-cells in series by their ability to power the LED. The voltage, current and LED data was then analysed using a range of appropriate equations to derive properties of the galvanic half-cells, such as power output, specific power, energy output, specific energy, and cell voltage, which can be compared to a theoretical value (Zn–Cu ~1.10 V). These equations include:

- Power output (watts): $P = V \times I$
  (P = power, V = voltage, I = current)
- Energy output (joules): $E = P \times t$
  (E = energy, P = power, t = time)

3. Results & Discussion

3.1: Effect of electrolyte concentration on voltage and current

In a half-cell, oxidation at the anode releases electrons that flow through an external wire to the cathode, where reduction occurs; ions migrate through the electrolyte to maintain charge balance.[7]

Anode (oxidation):
$Zn(s) \rightarrow Zn^{2+}(aq) + 2e^-$

Cathode (reduction):
$Cu^{2+}(aq) + 2e^- \rightarrow Cu(s)$

The net cell reaction is:
$Zn(s) + Cu^{2+}(aq) \rightarrow Zn^{2+}(aq) + Cu(s)$

The reaction has a theoretical standard cell potential of approximately 1.10 V, based on standard reduction potentials (E°) (Cu^{2+}/Cu = +0.34 V and Zn^{2+}/Zn = –0.76 V), under standard conditions: 1M concentrations, 25°C temperature, and 1 atm pressure. The initial experiment was to test how electrolyte concentrations of half cells would affect the voltage. Changing concentrations of both electrolytes didn't seem to largely affect the voltage. This minimal change is shown in Table 1.

Concentration of Zn^{2+}/Cu^{2+}	Voltage (V)
0.1M / 0.1M	1.0293
0.5 M / 0.5M	1.0408
1.0 M / 1.0M	1.0209
2.0M / 2.0M	0.9996

Table 1: Voltage readings under same concentrations of Zn^{2+}/Cu^{2+}

This trend suggests that the Nernst equation's concentration effect was relatively weak under our experimental setup, possibly due to factors such as electrode surface condition or limitations in our measurement precision.[8]

Further tests examined the effect of unequal concentrations between half-cells. Again, changes were minor, shown in Table 2.

Zn^{2+}	Cu^{2+}	Voltage (V)
0.1	2.0	1.0020
2.0	0.1	1.0212

Table 2: Voltage readings under same concentrations of Zn^{2+}/Cu^{2+}

The slightly higher voltage in the second case (more $Zn^{2+}$and less Cu^{2+}) could be due to the direction of the Nernst shift, which favors higher potential when the oxidized form (Zn^{2+}) is more concentrated and the reduced form (Cu^{2+}) is more dilute, therefore shifting the equilibrium potential of the reaction. However, these differences are minor and the observed voltages were consistently slightly lower than the theoretical 1.10 V, likely due to internal resistance like ohmic resistance, imperfect electrodes, or non-ideal conditions. [9]

While voltage remained fairly stable across concentrations, current output showed a small peak at 0.5 M, suggesting a subtle influence of ion availability on current flow.[10]

Concentration of Zn^{2+}/Cu^{2+}	Current (mA)
0.1M / 0.1M	0.270
0.5 M / 0.5M	0.283
1.0 M / 1.0M	0.265

Table 4: Voltage readings in different number series

These values suggest that there may be an optimal concentration (~0.5 M) where ion mobility and conductivity are most favorable. At lower concentrations (0.1 M), limited ions may restrict current flow, while at higher concentrations (1.0 M), increased ionic interactions or electrode

fouling may reduce efficiency slightly.

3.2: Effect of cell configuration on voltage

When multiple galvanic half cells were connected in series, their voltages added up approximately linearly.[11] This demonstrates the fundamental principle of series circuits in electrochemistry: total voltage is the sum of the individual cell voltages.[12] Shown in Table 4.

Configuration	Voltage (V)
One cell (0.1M)	1.0293
Two cells (0.1M and 1M)	2.0290
Three cells (0.1, 1M, and 2M)	3.0656

Table 4: Voltage readings in different series

When all three cells were placed in series, the cumulative voltage was enough to light up all the different colours of LEDs, each requiring a specific forward voltage with green being the highest at 3.0-3.2V and red being the lowest at 2.0-2.2V. This highlights the usefulness of series configurations for applications requiring higher voltages.[13]

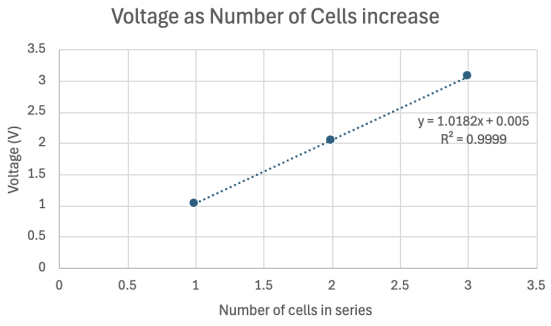

Figure 2: Graph of voltage against number of cells in series

There would be another way to increase the voltage generated with the same cell arrangement. This can be done through the use of an alkaline electrolyte for each half cell instead of a neutral electrolyte.[14] By increasing the alkalinity of the electrolyte, another path is formed for a more efficient flow cell battery system as there is an increase in the redox potential of the metals in electrolytes of higher pH values.[15] With this increased efficiency, comes various possible downsides which could affect the cell potential. There is a greater chance of precipitation of the metal and effervescence of hydrogen in higher pH conditions which would reduce the surface area of the electrodes and lead to drastic reductions in the rate of the redox reactions.[16]

3.2 Reducing low-grade energy waste

When operating with half-cells, large amounts of heat dissipation should be taken into account for various reasons. The heat that's released is a low-grade energy waste which plays a big role in the ongoing climate crisis.[17] Furthermore, efficiency is increased when heat loss is reduced which shows that there are environmental and economical benefits.[18]

A viable solution to reduce heat emitted from the cells would be to recycle the heat back into the system to further drive the redox reactions happening based on the thermally regenerative electrochemical cycle (TREC).[19] By installing a heat exchanger[20] between the 2 half-cells, the heat exchanger could be used to recover the heat dissipated throughout the process[21] that is brought about from factors such as the electrolyte flow across the cell and ohmic effect present at the electrodes of the cell. However, this would only be reasonable to apply if the galvanic cell is being utilised on a large scale. At a large scale, temperature of the electrolytes are raised to high levels hence causing there to be sufficient heat dissipation.[22] This allows for the addition of a heat exchanger as a significant amount of heat to be recycled back into the system and generate a much greater voltage so that the cost of the heat exchanger would be offset by the increased efficiency of the system on top of the positive environmental impact it will have.

3.3 Thermogalvanic cells

Building on what was previously mentioned and by adding an external natural heat source to the system, thermogalvanic single cells can be brought by the combined utilisation of both low-grade waste heat and the external heat source to generate larger voltage outputs and hence greater energy and power outputs too,[23] augmenting the sustainability factor of energy generation.[24] The primary driving power for electrolyte flow would be the natural heat source, which could be solar energy or geothermal energy, instead of the redox reactions. The heat source would heat the anode and hence cause a temperature gradient between the anode and cathode to be formed. The temperature gradient is maintained by the heat exchanger which would also act as a membrane between the half-cells to accommodate for ions to flow between the two half-cells. This gradient would generate a voltage which would supplement the voltage produced by the redox reactions occurring in the half cells to produce a larger combined voltage.

Utilising the capabilities thermogalvanic cells have to continuously generate electrical output[25] and the trends shown in *Figure 2*, voltage and electrical energy output can be further improved which is vital for developing countries which are in need of a large constant supply of electricity at minimal cost.[26]

4. Conclusion

This experiment shows how basic zinc-copper galvanic cells can generate electrical power and what factors affect their performance. It was found that varying the concentration of the electrolyte solutions had minimal impact on the voltage output. The result of the experiment was close to the initial value, with the voltage values being next to 1.0V, a bit less than the theoretical value of 1.10V. This small difference is thought to be due to internal resistance or other practical limitations within the system.

On the other hand, attaching a few more cells in series produced a considerable change in the total voltage. A total voltage of 3.07 V was produced with 3 interconnected cells, which was used to light LEDs of different colours. This experiment shows that basic electrochemical systems can be used to transform energy to produce larger requirements, which proves the real-world applicability. Additionally, there are ways to enhance the system's efficiency, like using alkaline electrolytes or applying thermally regenerative systems to recover heat. Thus, the ideas serve as an example that galvanic cells are not only instruments but also permit the use of renewable and affordable energy storage solutions.

In conclusion, all our theoretical topics were brought into the realm of real life, which has given birth to future developments leading to an improved design and innovation of battery technology.

Appendix

Zinc Concentration (M)	Copper Concentration (M)	Volts Direct Current (V)
2	0.1	1.0212
0.1	2	1.0020
2	2	0.9996
0.1	0.1	1.0293
1	1	1.0209
Two in series (0.1M, and 1M)		2.0290
Three in series (0.1M, 1M, 2M)		3.0656

Acknowledgements

Dinara Kalupahana was responsible for writing up the abstract and the introduction; Matyas Vyhnalek completed the materials and methods; Minh Tri Truong and Shael Caden Chandran composed the results and discussion; Rakeisha Heidi Liem formulated the abstract and conclusion. Benedict Tai, Jordan Kambanis and Masoomeh Asgharnejad-laskoukalayeh provided task direction and project assistance, Thomas Whittle designed the experiment, David Alam facilitated project resources and guidance on conceptual direction, and Gobinath Rajarathnam ideated conceptual direction, research and writing guiding frameworks, and direct project supervision.

The authors acknowledge the use of AI tools to assist with grammar checking, language refinement, and the retrieval of general information during the preparation of this work.

References

[1] Brett, C. M. A. Standard electrode potentials and application to characterization of corrosion phenomena. *ScienceDirect*, 511–516 https://doi.org/10.1016/B978-0-12-409547-2.13389-X (2018).

[2] Salameh, Z. Chapter 4 - Energy Storage. *ScienceDirect*, 201–298 https://doi.org/10.1016/B978-0-12-374991-8.00004-0 (2014).

[3] O. Østerberg, N. L. Sørensen, T. & A. Jensen, J. Practical and theoretical aspects concerning the use of salt bridges in electrochemistry. *Journal of Electroanalytical Chemistry and Interfacial Electrochemistry* **119**, (1981).

[4] Jain, S. & Kumar, L. Fundamentals of Power Electronics Controlled Electric Propulsion. *Power Electronics Handbook*, 1023–1065 https://doi.org/10.1016/b978-0-12-811407-0.00035-0 (2018).

[5] Wiegelmann, S., Bensmann, A. & Hanke-Rauschenbach, R. Performance characterization of lithium-ion battery cells within restricted operating range using an extended ragone plot. *Applied Energy* **389**, 125704 (2025).

[6] K. Maniam, K. & Paul, S. Electrodeposition for renewable energy applications. *Elsevier eBooks*, 521–531 https://doi.org/10.1016/b978-0-323-85669-0.00083-0 (2024).

[7] Torabi, F. & Ahmadi, P. Chapter 2 - Fundamentals of batteries. *ScienceDirect*, 55–81 https://doi.org/10.1016/B978-0-12-816212-5.00006-4 (2020).

[8] Vincent, C. & Scrosati, B. Modern Batteries. *ScienceDirect*, https://doi.org/10.1016/B978-0-340-66278-6.X5000-1 (1997).

[9] P. Kundu, P. & Dutta, K. Progress and Recent Trends in Microbial Fuel Cells. *ScienceDirect*, https://doi.org/10.1016/C2016-0-04695-8 (2018).

[10] Alberto Varone, Michele Ferrari, Power to liquid and power to gas: An option for the German Energiewende, *Renewable and Sustainable Energy Reviews*, 207-218 https://doi.org/10.1016/j.rser.2015.01.049 (2015).

[11] Ciobanu, M. P. Wilburn, J. L. Krim, M. E. Cliffel, D. Fundamentals. Handbook of Electrochemistry. *Elsevier*, 3-29 https://doi.org/10.1016/B978-044451958-0.50002-1 (2007)

[12] Xu, H. & Meng Ni, M. High-temperature electrolysis and co-electrolysis. Power to Fuel. *Academic Press*, https://doi.org/10.1016/B978-0-12-822813-5.00008-4 (2021).

[13] Madec, L. Martinez, H. Impact of the metal electrode size in half-cells studies. *Electrochemistry Communications*, 61-64 https://doi.org/10.1016/j.elecom.2018.04.007 (2018).

[14] Thamizhselvan, R., Naresh, R., Sekar, R., Ulaganathan, M., Pol, V. G. & Ragupathy, P. Redox flow batteries: Pushing the cell voltage limits for sustainable energy storage. *J. Energy Storage* https://doi.org/10.1016/j.est.2023.106622 (2023).

[15] A. Kulikovsky, A. Analytical Models of a Direct Methanol Fuel Cell. *Elsevier Science*, 337-417 https://doi.org/10.1016/S1752-301X(07)80011-1 (2007).

[16] N. Ueoka, N. Sese, M. Sue, A. Kouzuma, K. Watanabe, Sizes of anode and cathode affect electricity generation in rice paddy-field microbial fuel cells. *Journal of Sustainable Bioenergy Systems*, 1023-1065 https://doi.org/10.4236/jsbs.2016.61002 (2018).

[17] Nugraheni, E. & Agus, S. & Ari, R. The effect of configuration structure of lithium-ion battery: analysis

of the temperature distribution performance. *Journal of Physics* **2190**, https://iopscience.iop.org/article/10.1088/1742-6596/2190/1/012043 (2022).

[18] Forman, C., Muritala, I. K., Meyer, B., & Spliethoff, H. Estimating the global waste heat potential. *Energy Rev*, 1568–1579 https://doi.org/10.1016/j.rser.2015.12.192 (2016).

[19] Bleeker, J., Reichert, S., Veerman, J. *et al.* Thermo-electrochemical redox flow cycle for continuous conversion of low-grade waste heat to power. *Sci Rep* **12**, https://doi.org/10.1038/s41598-022-11817-1 (2022).

[20] Qian, X. Shin, J. Tu, Y. H. Zhang, J. & Chen, G. Thermally Regenerative Flow Batteries with pH Neutral Electrolytes for Harvesting Low Grade Heat. *Department of Mechanical Engineering MIT*, https://doi.org/10.48550/arXiv.2103.06243 (2021).

[21] Yin, C., Lu, M., Ma, Q., Su, H., Yang, W. ,& Xu, Q.A Comprehensive Flow- Mass-Thermal-Electrochemical Coupling Model for a VRFB Stack and Its Application in a Stack Temperature Control Strategy. *Batteries* **10**, https://doi.org/10.3390/batteries10100347 (2024).

[22] Furquan, M. M. Bhat, Z. Qamar, M. Electrolyte engineering beyond the conventional alkaline concentration for high-capacity retention of aqueous redox flow batteries. *Electrochimica Acta* **529**, https://doi.org/10.1016/j.electacta.2025.146286 (2025).

[23] Pavel, T. Polina, S. Liubov, N. The research of the impact of energy efficiency on mitigating greenhouse gas emissions at the national level. *Energy Conversion and Management* **314**, https://doi.org/10.1016/j.enconman.2024.118671 (2024).

[24] Chi, C. *et al*. Bioinspired Double-Layer Thermogalvanic Cells with Engineered Ionic Gradients for High-Efficiency Waste Heat Recovery. *Nano Energy* **111189**, https://doi.org/10.1016/j.nanoen.2025.111189 (2025).

[25] Yu, B. *et al*. All-Day Thermogalvanic Cells for Environmental Thermal Energy Harvesting. *Research (Wash D C)*, https://spj.science.org/doi/10.34133/2019/2460953 (2019).

[26]Burmistrov, I. *et al*. Advances in Thermo-Electrochemical (TEC) Cell Performances for Harvesting Low-Grade Heat Energy: A Review. *Sustainability*, **14**, 9483, https://doi.org/10.3390/su14159483 (2022).

The Sydney Journal of Interdisciplinary Engineering
SJIE 1(1) X–X (2025) https://doi.org/XXXX/XXXX

Construction and Optimisation of Zinc-Copper Galvanic Half-Cells with LED Illuminations

Raminus Samad Khan[1], Tahlia Robertson[1], Kushagr Gowda[1], Yash Makhija[1], Zachary Briscoe[1], Jordan Kambanis[1], Masoomeh Asghar Nejad-Laskoukalayeh[1], Benedict Tai[1], David Alam[1], Thomas Whittle[1] and Gobinath Rajarathnam[1]

[1] School of Chemical and Biomolecular Engineering, University of Sydney, Sydney, New South Wales, Australia

E-mail: rkha0681@uni.sydney.edu.au

Received xxxxxx
Accepted for publication xxxxxx
Published xxxxxx

Abstract

This study investigates the construction, performance, and optimisation of galvanic cells using copper-copper ion and zinc-zinc ion half-cells. The experiment aimed to explore electrochemical energy generation through redox reactions and to evaluate how design factors affect cell efficiency. Galvanic half-cells were assembled using 0.1 M and 0.05 M copper (II) sulfate and zinc sulfate solutions as standard electrolytes. Voltage and current outputs were measured with a multimeter, and the ability of each cell to power LEDs of different colours was assessed. Key variables, namely concentration, were systematically varied to determine their influence on electrical performance. The half-cell configuration demonstrated high output due to effective separation of half-reactions and minimal internal resistance. Increasing copper (II) sulfate concentration and decreasing zinc sulfate concentration generally improved performance, while series connections significantly boosted voltage, enabling the illumination of higher-threshold LEDs. The experiment highlighted the principles of electrochemical potential, circuit design, and redox chemistry. Results demonstrated the feasibility of using simple, low-cost materials to generate sufficient electrical energy for practical tasks such as lighting LEDs. This experiment emphasizes the relevance of electrochemical systems in sustainable energy applications and enhances understanding of real-world battery operation and optimisation.

Keywords: galvanic cell, zinc-copper cells, copper electrode, zinc electrode, redox reaction, electrolyte concentration, series and parallel connection

1. Introduction

Batteries are electrochemical devices, where electrical energy is generated from chemical energy by redox reactions at the anode and cathode, spontaneously[1]. Reactions at the anode, the negative electrode, generally take place at lower electrode potentials than at the cathode, the positive electrode. Batteries are closed systems, where the anode and cathode are the charge-transfer medium and are active reactants in the redox reaction. Thus, energy storage and conversion occur in the same compartment[2].

Galvanic cells, or voltaic cells, are the foundational models for electrochemical batteries. These cells generate electricity

spontaneously as electrons flow from the anode to the cathode[3]. This principle underpins the design of modern batteries used in portable electronics, electric vehicles, and renewable energy storage systems.

In galvanic cells the process is driven by a reduction in the change in Gibbs free energy, $\Delta_r G < 0$, as concentrations equilibrate[3]. In a typical galvanic cell, such as a zinc-copper system, zinc undergoes oxidation at the anode, releasing electrons and forming Zn^{2+} ions[4]. These electrons travel through an external wire to the cathode, where Cu^{2+} ions in solution are reduced to solid copper; this provides the electron flow of the system. A salt bridge connects the two half-cells, allowing ion transfer to maintain electrical neutrality and complete the internal circuit.

The schematic below illustrates how galvanic cells work, measuring the voltage of the cell using a voltmeter. The zinc anode and copper cathode are immersed in their electrolytes (Cu in Cu^{2+} ions and Zn in Zn^{2+} ions) and connected externally by a conductor and internally by a salt bridge soaked with potassium chloride (KCl) solution. Electron flow from the anode to the cathode generates usable electrical energy measured through the voltmeter, while ion movement through the salt bridge sustains the reaction.

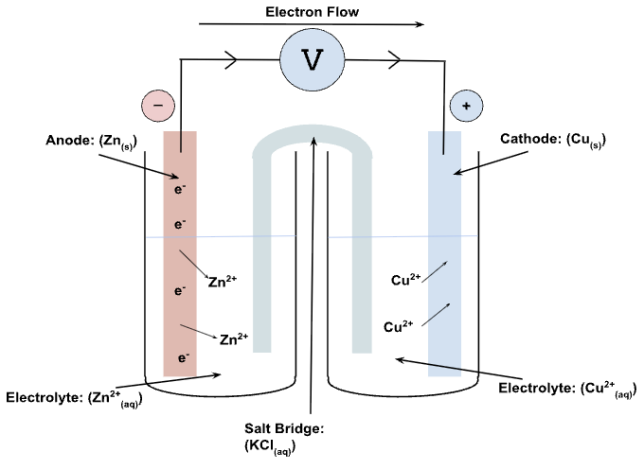

Figure 1: *Schematic diagram of a zinc-copper galvanic cell*

From an engineering standpoint, battery design involves optimising materials, reaction kinetics, and system integration, minimizing costs whilst maximizing efficiency and safety. Applications of electrochemistry are widespread in society, ranging from consumer electronics to automobiles, medical electronics and space travel. Electrode and electrolyte materials must be chosen by engineers for their conductivity, stability, cost, and environmental impact. Through thermodynamic properties such as cell potential and Gibbs free energy, energy output is determined, while kinetic factors influence charge and discharge[5]. Engineers must also address thermal management, mechanical durability, and safety, especially in large-scale or high-performance applications. Innovations such as lithium-ion, solid-state, and flow batteries have emerged and been optimised by the work of chemical engineers in combination with other engineering disciplines. Through this study we aim to explore how galvanic cells can be optimised to improve performance and efficiency, emulating how batteries are optimised industrially by chemical engineers.

2. Methods

2.1 Materials and Reagents

Copper (Cu) and Zinc (Zn) foils (cut to 3 cm × 6 cm) were used as electrodes. Initially, 0.1 M aqueous electrolyte solutions were prepared using distilled water, copper (II) sulfate ($CuSO_4$), zinc sulfate ($ZnSO_4$) solutions. Cotton rope strips were used to prepare salt bridges and spacers. Centrifuge tubes served as individual half-cell containers. Electrical measurements were taken using a digital multimeter. Alligator clips and insulated wires facilitated connections. Light-emitting diodes (LEDs) of different colours (green, blue, white, yellow, red) were used for output tests.

2.2 Preparation of Electrodes and Electrolytes

Copper and zinc foils were abraded with fine sandpaper to ensure a clean, reactive surface for the half-cell. Electrolyte solutions were prepared at 0.1 M and 0.05 M concentrations. Salt bridges were created by soaking cotton rope strips in 0.1 M potassium chloride (KCl) solution.

2.3 Construction of Galvanic Cells

Two centrifuge tubes were used as the basis of the half-cells. One was filled to two-thirds capacity with 0.1 M $CuSO_4$ and the other with 0.1 M $ZnSO_4$. A sanded copper electrode was placed in the $CuSO_4$ solution (cathode), and a sanded zinc electrode in the $ZnSO_4$ solution (anode). The half-cells were connected using the salt bridge prepared by cotton rope strips soaked in 0.1 M KCl. Electrodes were connected to a multimeter using alligator clips to measure electrical output. This process was repeated with different combinations of concentrations of $CuSO_4$ and $ZnSO_4$ to make four galvanic cells.

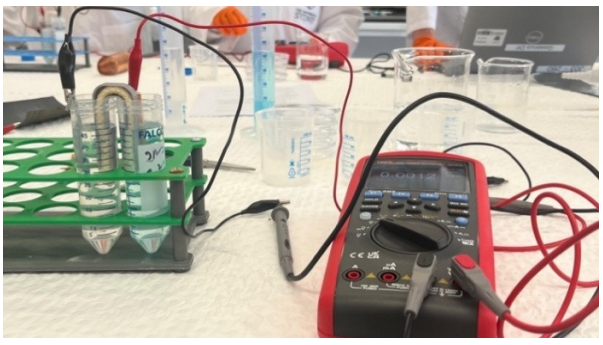

Figure 2: *Zinc-Copper Galvanic Cell Experimental Setup*

2.4 Series and Parallel Configurations

The galvanic cells were connected in series to find the optimal configuration to illuminate different LEDs. Voltage across the terminal ends and current in the circuit were measured for each successful configuration using a digital multimeter. The galvanic cells were not connected in parallel as it would not yield enough electromotive force (E.M.F.) to illuminate the LEDs.

2.5 Data Collection

Two forms of data collection were carried out. The first was electrical measurements, where voltage was measured under open-circuit conditions and the short-circuit current was measured by switching the multimeter to current mode. The second data collection was qualitative, LED lighting. Each cell configuration (series, parallel) was connected to a circuit containing one LED at a time, in the sequence: green → blue → white → yellow → red. LEDs were observed for illumination, and the results were recorded

2.6 Investigation of Variable Parameters: Electrolyte Concentration

Electrolyte concentrations of $CuSO_4$ or $ZnSO_4$ solutions varied as both the electrolytes were prepared with 0.1 M and 0.05 M concentrations. Multiple galvanic cells were constructed using the modified parameter while keeping other conditions constant. Voltage and current outputs were measured for each variation.

2.7 Data Analysis

Voltage and current data were analysed to determine trends related to cell configuration (single, series, parallel), parameter variation (electrolyte concentration), and LED illumination threshold. Trends were graphed to show relationships between variables. Observations on LED illumination were linked to measured output values to determine minimum requirements for successful operation.

2.8 Equations and Standard Potentials

The net reaction of a copper-zinc galvanic cell is,

$$Zn_{(s)} + Cu^{2+}{}_{(aq)} \rightarrow Zn^{2+}{}_{(aq)} + Cu_{(s)}$$

Oxidation at anode (Zn^{2+}/Zn half-cell):

$$Zn_{(s)} \rightleftarrows Zn^{2+}{}_{(aq)} + 2e-$$

Reduction at cathode (Cu^{2+}/Cu half-cell):

$$Cu^{2+}{}_{(aq)} + 2e- \rightleftarrows Cu_{(s)}$$

The theoretical cell potential, E^{o}_{cell}, is calculated as,

$$E^{o}_{cell} = E^{o}_{cathode} - E^{o}_{anode}$$

Where, $E^{o}_{cathode}$, standard reduction potential of cathode (Cu^{2+}/Cu), is +0.34V and E^{o}_{anode}, standard reduction potential of anode (Zn^{2+}/Zn), is −0.76V [6].

Thus, E^{o}_{cell} = +0.34 V – (–0.76 V) = +1.10 V [7].

2.9 Safety and Waste Disposal

All chemical handling was performed with gloves and safety goggles. Toxic solutions such as $CuSO_4$ were disposed of in heavy metal waste containers. Direct skin contact with $ZnSO_4$ was avoided. Electrical testing was conducted using insulated wires and connectors.

3. Results and Discussion

3.1 Results

Table 1: *Cell potential with different combinations of electrolyte concentrations*

Battery	[$CuSO_4$] (M)	[$ZnSO_4$] (M)	Cell Potential, E_{cell}, (V)
A	0.10	0.10	1.0652
B	0.10	0.05	1.0707
C	0.05	0.05	1.0545
D	0.05	0.10	1.0480

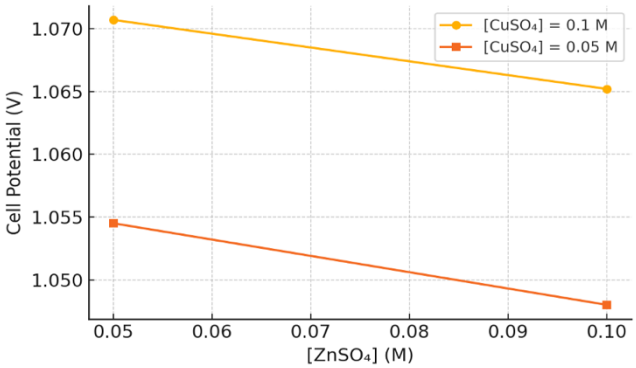

Figure 3: *Graph of how the cell potential varies with different combinations of electrolyte concentrations (Generated by AI using the raw data from the experiment)*

Table 2: *Electromotive Forces across the circuit for Different LEDs*

Colour of LED	Wavelength of LED (nm)	Series Connection of Batteries	E.M.F. (V)
Red	622.5	A + B	2.1296
Yellow	592.5	A + B	2.1323
White	550.0	A + B + C	3.1689
Blue	462.5	A + B + C	3.1857
Green	522.5	A + B + C	3.1887

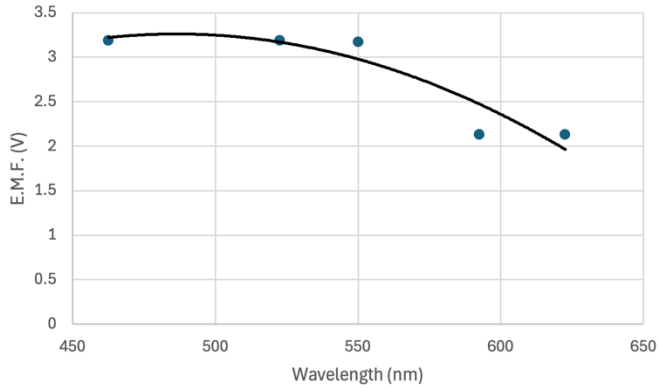

Figure 4: *Graph of how the E.M.F.varies across different wavelengths*

Table 3: *Current in the circuit for Different LEDs*

Colour of LED	Wavelength of LED (nm)	Series Connection of Batteries	Current (mA)
Red	622.5	A + B	19.831
Yellow	592.5	A + B	19.350
White	550.0	A + B + C	19.953
Blue	462.5	A + B + C	19.880
Green	522.5	A + B + C	19.802

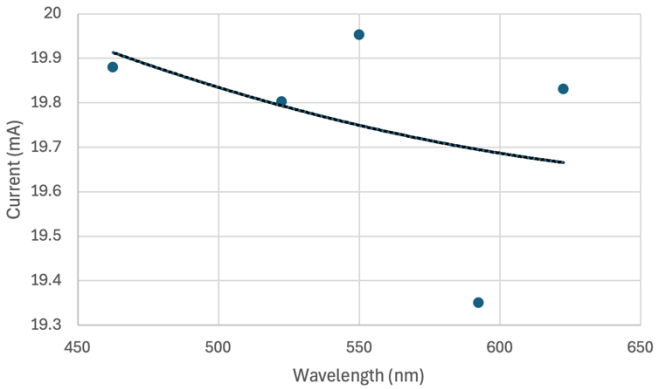

Figure 5: *Graph of how the current varies across different wavelengths*

Table 4: *Power output by the series connection of batteries for illuminating different LEDs*

Colour of LED	Wavelength of LED (nm)	Series Connection of Batteries	Power Output (mW)
Red	622.5	A + B	42.232
Yellow	592.5	A + B	41.260
White	550.0	A + B + C	63.229
Blue	462.5	A + B + C	63.332
Green	522.5	A + B + C	63.142

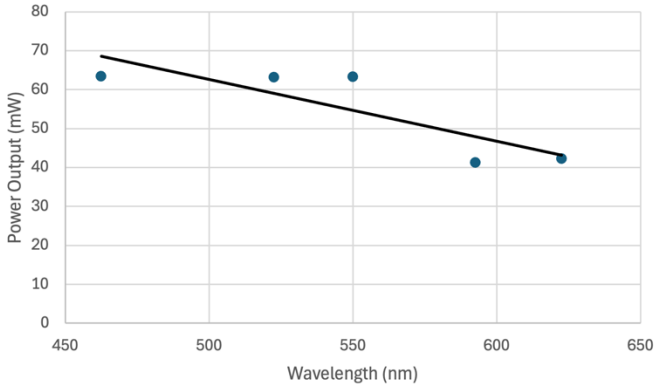

Figure 6: *Graph of how the power output varies across different wavelengths*

Table 5: *Energy output in 5 seconds and specific power for illuminating different LEDs*

Colour of LED	Wavelength of LED (nm)	Series Connection of Batteries	Energy Output in 5 seconds (mJ)	Specific Power (Wm^{-2})
Red	622.5	A + B	211.16	23.462
Yellow	592.5	A + B	206.30	22.922
White	550.0	A + B + C	316.15	35.127
Blue	462.5	A + B + C	316.66	35.184
Green	522.5	A + B + C	315.71	35.079

3.2 Discussion

Electrical measurements of galvanic cells are a direct method to evaluate their electrochemical performance by quantifying voltage, current, and power output under varying conditions, such as electrolyte concentration. At an electrolyte concentration of 0.1 M $CuSO_4$ and 0.1 M $ZnSO_4$ produced a cell potential of +1.0652 V which is in line with the theoretical value of +1.10 V, thus confirming that the fundamental electrochemical reaction being conducted is

$$Zn_{(s)} + Cu^{2+}{}_{(aq)} \rightarrow Zn^{2+}{}_{(aq)} + Cu_{(s)}$$

In the galvanic cell, oxidation occurs at the zinc anode as zinc is oxidised to Zn^{2+} ions following the half-cell equation, $Zn_{(s)} \rightleftarrows Zn^{2+}{}_{(aq)} + 2e-$, and reduction at the copper cathode as Cu2+ ions are reduced to copper following the half-cell equation, $Cu^{2+}{}_{(aq)} + 2e- \rightleftarrows Cu_{(s)}$.

3.2.1 Effect of Electrolyte Concentration

Systematic variation of electrolyte concentrations of 0.05 M and 0.1 M shows that changing $CuSO_4$ and $ZnSO_4$ concentrations affected cell potential and current output. This observation is consistent with the Nernst equation, where due to Le Chatelier's principle, a higher concentration of Cu^{2+} ions shifts the equilibrium to favour the reduction pathway (https://link.springer.com/article/10.1007/bf02645347).

$$E_{cell} = E°_{cell} - \frac{RT}{nF} \ln ([Zn^{2+}] / [Cu^{2+}])$$

The Nernst equation[8] shown above mathematically describes the relationship between the cell potential, temperature, and the concentrations of the involved ionic species. Thus, it shows the nonlinear impact of concentration changes on voltage output[9].

The Nernst equation[10] contains a natural logarithm. As a result, small changes in the concentration of electrolytes have a nonlinear but significant effect on the cell potential[11]. Thus, if the $[Cu^{2+}]$ decreases, the cell potential read by the multimeter will be lower as the cathode has fewer available ions to reduce, hence the reduction pathway becomes less favourable and thus the cell potential drops. This is evidenced by the data, as in both the galvanic cells with the $[Cu^{2+}]$ being 0.05 M, the E_{cell} values are lower than the E_{cell} values of the galvanic cells where $[Cu^{2+}]$ was 0.1 M, with the latter being 1.0480V at its lowest, and the former at 1.0707V at its highest. However, with reference to the Nernst equation, lower Zn^{2+} ion concentration makes the oxidation reaction more thermodynamically stable, as this favours the oxidation pathway, thus raising the cell potential.

3.2.2 Connecting Cells in Series and Parallel Configurations

The effects of connecting multiple cells in series and parallel were also examined. When cells are connected in series, cell potentials add linearly to give the electromotive force (E.M.F.) across the circuit[12]. Three galvanic cells in a series connection yielded an electromotive force (E.M.F.) of approximately 3.19 V, which was sufficient to illuminate LEDs with higher forward voltage thresholds such as white, blue, and green. This is evidenced by higher threshold LEDs such as white, blue, and green requiring three galvanic cells for activation, whereas red and yellow LEDs were illuminated by two cells connected in series. This is in line with their known forward voltages ranging from 2.0 V to 2.2 V for red and yellow LEDs and 3.0 V to 3.2 V for white, blue and green LEDs.

While not tested in this experiment, cells may also be connected in parallel. This, in essence, will result in the electromotive force (E.M.F.) of the circuit to be the same as the cell with the highest cell potential[13]. However, it will increase the current capacity greatly, thus improving runtime. However, parallelly connecting three cells with E.M.F. values of approximately 1.10 V will not be sufficient to power the LEDs due to their forward voltages ranging from 2.0 V to 3.2 V.

It is important to mention that current measurements were consistently conducted at the conclusion of each trial, as initiating current flow earlier would result in the immediate depletion of the cell, thereby preventing further experimentation. This rapid discharge is characteristic of series circuits, where the same current flows through each cell, leading to increased total energy consumption. In such configurations, there exists only a single path for the electric current, which imposes a uniform and continuous load across all cells. By contrast, in parallel circuits, the total current is distributed among the individual branches[14], thereby reducing the load experienced by each cell and extending the overall runtime of the battery system. This distinction arises from fundamental circuit behaviour, wherein parallel arrangements reduce effective resistance and distribute current more efficiently as current is divided amongst cells[15], reducing the load on the battery, resulting in slower depletion rates.

3.2.3 Trends Observed in the Recorded and Calculated Data and Battery Performance Analysis

While both the electromotive force (E.M.F.) across the circuit and current in the circuit are observed to have a nonlinear decreasing trend, the shape of the best-fit curve for both their trends are very different. However, the trends are difficult to observe as the red and yellow LEDs had the same forward voltage ranges, the white, blue and green LEDs had the same forward voltage ranges, and all the LEDs had the same maximum current.

However, the power output by the series connection of the batteries shows a linear decreasing trend across the wavelengths.

To evaluate the performance of the constructed battery systems, specific power and energy output in 5 seconds were calculated and analysed. Specific power refers to the rate at which energy is delivered per unit area of the electrode. In the highest-performing configuration (white LED, three cells in series), a specific power of approximately 35.13 W/m² was recorded, along with an energy output of 316.15 mJ over 5 seconds. These values, while shy in performance to commercial batteries, demonstrate the cell's capability to deliver targeted power outputs for low-energy applications.

3.2.4 Zinc-Copper Galvanic Cells in Engineering Context

Design and testing of copper-zinc galvanic cells presents implications for broad real-world applications, such as developing cost-effective yet sustainable energy storage solutions. Such simple cells exemplify the challenges encountered in scaling up electrochemical systems. For example, low energy density, relatively short lifespan due to reactant depletion, and limitations in voltage output from single cells to name a few. However, the results also highlight the advantages of reconfigurability, where stacking and arranging cells in series or parallel configurations improves performance.

In resource-limited or remote settings, such as off-grid locations, galvanic cells offer a compelling option due to the accessibility of the materials as well as its ease of

assemblance. In industrial settings, however, cost-performance trade-offs are a crucial consideration. Whilst zinc-copper galvanic cells may not outperform lithium-ion electrochemical technologies on energy density or life cycle, they are however low cost, environmentally friendly[16], and have safer operation conditions which make them more ideal for temporary applications, such as low-power environmental sensors or single-use diagnostic devices. The combination of safety, environmental sustainability and abundant reserve make these energy storage systems highly advantageous for the environment[17].

From a sustainability perspective, using recyclable metals like copper and zinc and aqueous electrolytes poses less environmental risk than organic solvents to align these systems with greener energy production. Further research could optimize systems by exploring biodegradable electrolytes, waste-metal sourcing, or integration with renewable inputs. Moreover, zinc and copper can be recycled in economically feasible methods[18] to further improve its economic efficiency.

3.2.5 Possible Improvements in the Cell Design

Possible improvements in the zinc-copper galvanic cell can be brought about by significantly improving the specific energy by optimizing the electrode-to-electrode ratio and reducing internal resistance through better separation and increased ionic conductivity[19] and by increasing the energy density of the cell by increasing electrode thickness[20]. Further trial and error can be performed to find the optimal electrolyte configurations with different liquids as electrolytes with salt and other compounds to obtain optimal energy output[21].

Additionally, the zinc-copper galvanic cell can be improved by using optimised electrode configurations with accordance to their electrode architecture and improved fabrication strategies[22]. Furthermore, zinc-copper cells can be made rechargeable using a cation-exchange membrane to separate the half-cells with a sodium-based background electrolyte[23] or using electrolytes made from hydrogels[24] while increasing the output voltage of the cells by inserting two pairs of both cathodes and anodes in one volume of the electrolyte[25].

Such metrics are crucial in engineering design, particularly when selecting battery types for portable medical or environmental monitoring devices. As observed, even simple aqueous-based electrochemical cell designs can be tuned through their variable concentration and configurations to meet specific voltage and power requirements.

4. Conclusion

This experiment successfully demonstrated the principles of galvanic cell operation using copper and zinc electrodes, with variable electrolyte concentrations and cell configurations. The results followed expected trends, such as higher voltages from series connections and variable concentrations on output, thus reflecting how chemical potential and circuit design interplay in real world electrochemical systems.

Moreover, series connections significantly increased cell voltage, illuminating LEDs with higher voltage requirements. In contrast, changes in electrolyte concentration influenced cell voltage in a non-linear manner, small increases in Cu^{2+} ion concentration led to voltage gains, whereas small increases in Zn^{2+} ion concentration suppressed voltage, staying consistent with the Nernst equation. Power values reached over 35 W/m² in the most efficient configuration, suggesting feasibility of such cells for low-power applications.

These findings are relevant for developing accessible and sustainable battery technologies that prioritize safety, low cost, and reconfigurability. Further improvements could explore more materials, higher electrode surface areas, and hybrid integration of cells with renewable energy systems. The experiment reinforces the role of electrochemical engineering in tackling modern energy challenges and provides a foundation for future innovation in battery design.

Acknowledgements

We thank Dr. Gobinath Rajarathnam for his supervision, ideation of conceptual direction and intellectual input. We thank Dr David Alam and Dr Thomas Whittle for their intellectual inputs in the experiment. We thank Benedict Tai, Jordan Kambanis and Masoomeh Asghar Nejad-Laskoukalayeh for their supervision and intellectual input. The authors acknowledge the use of AI for generating a graph from raw experimental data.

Authorship Statement

Raminus Samad Khan conducted the experiment, recorded the raw data, prepared the results, research and writing cell design improvements, incorporated all sections of the article, and performed complete article modeling; Tahlia Robertson conducted the experiment, research on the experiment, and writing the abstract and methods; Kushagr Gowda conducted the experiment, research and writing the discussion; Yash Makhija conducted the experiment, research and writing the discussion and the conclusion; Zachary Briscoe conducted the experiment, research and writing the introduction; Benedict Tai, Jordan Kambanis and Masoomeh Asghar Nejad-Laskoukalayeh provided task direction and project assistance; Dr Thomas Whittle designed the experiment; Dr David Alam facilitated project resources and guidance on conceptual direction; and Dr. Gobinath Rajarathnam ideated conceptual direction, research and writing guiding frameworks, and direct project supervision.

References

1 Petrovic, S. & Petrovic, S. Galvanic Cells. *Electrochemistry Crash Course for Engineers*, 77-83 (2021).

2 Winter, M. & Brodd, R. J. What Are Batteries, Fuel Cells, and Supercapacitors? *Chemical Reviews* **104**, 4245-4270 (2004). https://doi.org/10.1021/cr020730k

3 Schmidt-Rohr, K. How Batteries Store and Release Energy: Explaining Basic Electrochemistry. *Journal of Chemical Education* **95**, 1801-1810 (2018). https://doi.org/10.1021/acs.jchemed.8b00479

4 Lower, S. K. Chemical reactions at an electrode, galvanic and electrolytic cells. *Electrochemistry; Simon Fraser University: Burnaby, BC, Canada*, 35-38 (2004).

5 Fuller, T. F. & Harb, J. N. *Electrochemical engineering*. (John Wiley & Sons, 2018).

6 Kumar, R. V. & Sarakonsri, T. Introduction to electrochemical cells. *High energy density lithium batteries: materials, engineering, applications*, 1-25 (2010).

7 Elsener, B., Andrade, C., Gulikers, J., Polder, R. & Raupach, M. Half-cell potential measurements—Potential mapping on reinforced concrete structures. *Materials and Structures* **36**, 461-471 (2003).

8 Vidal-Iglesias, F. J., Solla-Gullón, J., Rodes, A., Herrero, E. & Aldaz, A. Understanding the Nernst Equation and Other Electrochemical Concepts: An Easy Experimental Approach for Students. *Journal of Chemical Education* **89**, 936-939 (2012). https://doi.org/10.1021/ed2007179

9 Rajesh, A. Effect of Electrolyte Concentration on the Efficiency of Electrochemical Cells in India. *Journal of Chemistry* **3**, 31-41 (2024). https://doi.org/10.47672/jchem.2402

10 Feiner, A. S. & McEvoy, A. J. The Nernst Equation. *Journal of Chemical Education* **71**, 493 (1994). https://doi.org/10.1021/ed071p493

11 Hahn, N. T. *et al.* Concentration-dependent ion correlations impact the electrochemical behavior of calcium battery electrolytes. *Physical Chemistry Chemical Physics* **24**, 674-686 (2022).

12 Oliot, M., Etcheverry, L., Mosdale, R. & Bergel, A. Microbial fuel cells connected in series in a common electrolyte underperform: understanding why and in what context such a set-up can be applied. *Electrochimica Acta* **246**, 879-889 (2017).

13 Hofmann, M. H. *et al.* Dynamics of current distribution within battery cells connected in parallel. *Journal of Energy Storage* **20**, 120-133 (2018). https://doi.org/https://doi.org/10.1016/j.est.2018.08.013

14 Paul, C. R. *Fundamentals of electric circuit analysis*. (John Wiley & Sons, 2001).

15 Imtiyaaza, K. A. *et al.* Analyzing Ohm's Law: Comparison of Current and Resistance in Series and Parallel Circuits. *Schrödinger: Journal of Physics Education* **5**, 142-149 (2024).

16 Amayreh, M. A. Low-cost, environmentally friendly galvanic cells. *Chemist* **93**, 1-10 (2022).

17 Zhu, X. *et al.* A self-optimized dual zinc/copper-electrolyte anodic interfaces by mechanical rolling toward zinc ion batteries with high capacity and long cycle life. *Materials Today Energy* **23**, 100897 (2022). https://doi.org/https://doi.org/10.1016/j.mtener.2021.100897

18 van Beers, D., Kapur, A. & Graedel, T. E. Copper and zinc recycling in Australia: potential quantities and policy options. *Journal of Cleaner Production* **15**, 862-877 (2007). https://doi.org/https://doi.org/10.1016/j.jclepro.2006.06.023

19 Raza, B. *et al.* Advances in Organic electrolytes for High-Performance zinc Batteries: Enhancing zinc anode Robustness and efficiency. *Chemical Engineering Journal* **515**, 163617 (2025). https://doi.org/https://doi.org/10.1016/j.cej.2025.163617

20 Heubner, C., Langklotz, U. & Michaelis, A. Theoretical optimization of electrode design parameters of Si based anodes for lithium-ion batteries. *Journal of Energy Storage* **15**, 181-190 (2018). https://doi.org/https://doi.org/10.1016/j.est.2017.11.009

21 III, F. B. C., Cioco, J. M., Conge, L. R. & Gadin, A. U. Design, Testing, and Construction of an Alternative Zn-Cu Electrolytic Cell Battery. *Journal of Academic Research* **4**, 21-31 (2019).

22 Jeong, B., Ocon, J. D. & Lee, J. Electrode architecture in galvanic and electrolytic energy cells. *Angewandte Chemie International Edition* **55**, 4870-4880 (2016).

23 Jameson, A., Khazaeli, A. & Barz, D. P. J. A rechargeable zinc copper battery using a selective cation exchange membrane. *Journal of Power Sources* **453**, 227873 (2020). https://doi.org/https://doi.org/10.1016/j.jpowsour.2020.227873

24 Mypati, S., Khazaeli, A. & Barz, D. P. J. A novel rechargeable zinc–copper battery without a separator. *Journal of Energy Storage* **42**, 103109 (2021). https://doi.org/https://doi.org/10.1016/j.est.2021.103109

25 Lacina, K., Sopoušek, J., Skládal, P. & Vanýsek, P. Boosting of the output voltage of a galvanic cell. *Electrochimica Acta* **282**, 331-335 (2018). https://doi.org/https://doi.org/10.1016/j.electacta.2018.06.080

SJIE 1(1) X–X (2025) https://doi.org/XXXX/XXXX

Comparing Electrical Performance of Zn-Cu Flat Stacked and Rolled Galvanic Cells

Manas Srinivas, Emily Sewell, Lucas Sidney, Jacinta Wilkin, Bryan Law, Jordan Kambanis, Masoomeh Asghar Nejad-Laskoukalayeh, Benedict Tai, David Alam, Thomas Whittle, Gobinath Rajarathnam

School of Chemical & Biomolecular Engineering

E-mail:

Received xxxxxx
Accepted for publication xxxxxx
Published xxxxxx

Graphical Abstract

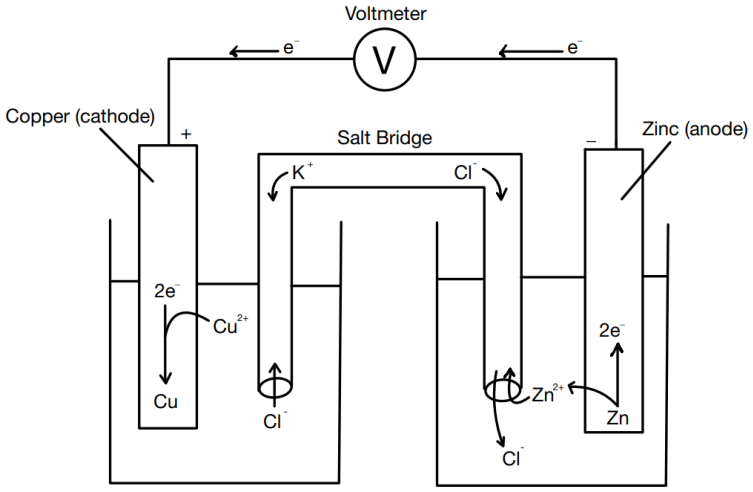

Figure 1. A standard zinc-copper galvanic cell

Abstract

Galvanic cells generate electricity from spontaneous redox reactions and are applied by chemical engineers in areas such as corrosion control and electroplating. This study investigates the electrochemical performance of zinc-copper (Zn-Cu) galvanic cells in flat-stacked and rolled configurations, isolating the influence of configuration on voltage, current and power output. Using a 0.1M KCl salt bridge with 6cm x 3cm copper and zinc electrodes, the cell output was measured. Furthermore, the effect of $ZnSO_4$ concentration (0.1M, 1M, 2M) was also tested. Rolled cells showed slightly higher voltage and current outputs, due to more effective electrode contact, however, both designs produced voltages below the theoretical 1.10V potential, due to current leakage, short circuits and lack of copper ions for cathodic reduction, increasing $ZnSO_4$ concentrations correlated with a decreasing cell voltage, aligning with predictions derived from the Nernst Equation. While the investigation generated reasonable results, deviations from theoretical values and measurement inconsistencies suggested experimental refinement is needed. The investigation provided insights into how cell geometry and electrolyte composition influence galvanic cell efficiency, providing insights into optimisation of electrochemical systems and contributing to sustainability in applications including energy storage and usage in electric vehicles and renewable energy storage[1].

Keywords: galvanic cells, zinc-copper battery, rolled cell, flat-stacked cell, electrolyte concentration, power density, Nernst equation

1. Introduction

A galvanic cell is an electrochemical device which is used to produce electricity through a spontaneous redox reaction. The anode is composed of a compound with a low reduction potential, being readily oxidised to generate electrons which flow through an external wire to the cathode, facilitating the reduction of the cathode and generating an electrical current[2]. The electrodes are submerged in an electrolyte solution, allowing the movement of ions, and maintaining neutrality within the cell. Batteries may contain one or more galvanic cells, converting chemical energy into electrical energy to fuel electric vehicles, phones, and off-grid renewable energy systems.

The application of a galvanic cell depends on the properties of the specific configuration utilised, including rolled, flat-stacked and half-cell designs. Rolled cells are very compact, and compared to flat stacked cells, they feature spiralled electrodes to increase the surface area for electron transfer, enhancing energy and power density[3]. This design, seen in commercial formats like AA and 18650 batteries, offers scalability, thermal stability, and ease of production, making it ideal for EVs and portable electronics[4], however, their stress concentrations may accelerate degradation. Flat-stacked cells, by contrast, use layered electrodes in a compact prismatic format, giving them better space utilisation and more uniform pressure distribution[5]. While more challenging to manufacture due to alignment precision and contamination risks, flat-stacked designs deliver superior structural performance and offer better energy efficiency.

Zinc, being higher in the reactivity series compared to copper, displaces copper ions from the solution, depositing them as solid copper, leading to the oxidation of zinc. Hence, in a closed circuit, a current flows between the two electrodes, where zinc acts as the anode (supplying electrons) and copper acts as the cathode (consuming electrons)[6], where the mass of the copper electrode increases. Copper and zinc electrodes, when immersed in electrolyte[7], create an electrochemical cell which generates electrical energy through a redox reaction. This process involves the oxidation of zinc to form positive Zn^{2+} and $2e^-$, and the reduction of copper to form metallic copper from the consumption of electrons. The half-cell equations are shown below:

$$Zn(s) \rightarrow Zn^{2+}(aq) + 2e^-$$
$$Cu^{2+}(aq) + 2e^- \rightarrow Cu(s)$$

For the comparison of the rolled cell and flat cell, a 0.1M KCl solution was chosen as the electrolyte. To determine the impact of concentration on the cell output, the concentration of a $ZnSO_4$ electrolyte was changed under a flat cell configuration, and the output was recorded. The electrodes are responsible for influencing the power output of the cell (i.e. the rate at which chemical energy is transformed into electrical energy), and this is dependent on the surface area and material of the electrode. A larger surface area exposes a larger number of atoms to the electrolyte mixture, meaning the metallic atoms in the electrode can be oxidised into ions at a greater rate, thus increasing the power output[8]. Furthermore, the reduction potential of a material will also influence the power. Anodes with a lower reduction potential will be oxidised more efficiently, and when paired with a cathode with a higher reduction potential (easily reduced), the rate of the redox reaction is greater, increasing the efficiency and power output of the cell[9].

Galvanic cells, while conventionally used as batteries, are now being used in the medical and environmental industries. Magnesium-based galvanic cells (MgG) are being used as a non-invasive tumour treatment as gas therapy. It involves micro-scale MgG rods being inserted into a tumour, with the Mg oxidised in the presence of water, forming both hydrogen gas and magnesium hydroxide[10].

$$Mg_{(s)} + 2H_2O_{(l)} \rightarrow H_{2\,(g)} + Mg(OH)_{2\,(aq)}$$

The hydrogen gas continuously produced induces mitochondrial dysfunction (by interfering with the electron transport chain) and impedes the maintenance of intracellular homeostasis. Furthermore, the $Mg(OH)_2$ can neutralise the acidic tumour environment. This helps to reduce toxicity on healthy cells and prevents the degradation of the extracellular matrix, thus preventing the spread of the tumour cells[11].

2. Experimental Aim

To build and compare different types of Zinc-Copper galvanic cells, including flat and rolled cells, to compare their properties regarding voltage and current output and the ability to light up different coloured LEDs. To investigate the effect of electrolyte concentration on voltage output.

3. Materials & Methods

3.1 Materials

A zinc-copper electrode was employed for the galvanic cell design, the copper foil acting as the cathode and the zinc foil acting as the anode. Alligator clips and wires were used to close the circuit, connecting the electrodes to all other circuit components, including the AAA batteries and LEDs. Filter paper acted as the salt bridge within the galvanic cell with the use of a 0.1M KCl solution, maintaining neutrality within the cell and facilitating electron movement throughout the circuit. Different-coloured LEDs (green, blue, white, yellow, and red) were used to test the output of the galvanic cell design by changing the energy requirement from the cell. A multimeter was used to measure the voltage and current output of the cell. Finally, beakers were used to hold samples of the salt bridge solutions, the petri dish was used to soak the filter paper in the salt bridge solution, with tweezers were used to transport the soaked filter paper from the petri dish. Scissors were used to cut the sheets of copper and zinc into 3cm x 6cm strips, and tape was used to hold the rolled galvanic cell securely shut.

3.2 Method

The copper and zinc sheets were cut into 2 separate 3cm x 6cm strips. Two sheets of filter paper were then cut into 3cm x 6cm strips (as flush to the electrodes as possible to prevent the circuit from shorting). Approximately 30 mL of the 0.1M KCl solution was poured from the beaker into the petri dish, and one strip of filter paper was placed into the petri dish to soak. Tweezers were used to remove the filter paper from the petri dish, which was sandwiched between the copper and zinc electrodes. Tape was

then used to secure the stacked cell into a cylindrical rolled configuration (Figure 2). Separate alligator clips and wires were clamped onto each electrode, where the zinc electrode was connected to the negative (black) probe of the multimeter, and the copper electrode was connected to the positive (red) probe, creating a series circuit. The multimeter was switched to V mode, and the voltage was measured before being switched to mA mode to record the current. The alligator clip was disconnected from the positive terminal of the multimeter, and a new alligator clip was connected to the positive terminal of the green light bulb. Another wire with an alligator clip was used to close the circuit, connecting the negative terminal of the light bulb with the positive terminal of the multimeter. A battery was then added in series, and following this, a second battery was added in series, directly in contact with the previous battery. The voltage and current were then recorded. The green light bulb was removed from the circuit and replaced with the blue light bulb, again measuring the voltage and current**.** This step was repeated for the white, yellow and red light bulbs, recording each voltage.

The second strip of filter paper was soaked in the petri dish with the 0.1M KCl solution, and the filter paper was placed between the second zinc and copper strips, creating a flat cell (Figure 2). An alligator clip was used to connect the positive probe of the multimeter to the copper electrode, while another wire and alligator clip were used to connect the zinc electrode to the negative multimeter probe. The initial voltage and current were then recorded. The green light bulb was then connected in series, disconnecting the alligator clip from the positive multimeter terminal, and connecting it to the positive terminal of the green light bulb before closing the circuit by using a new wire to connect the negative terminal of the light bulb to the positive multimeter probe. 2 batteries were added to the circuit in series. The green light was replaced with the blue, white, yellow then red light bulb, testing its ability to light up each colour.

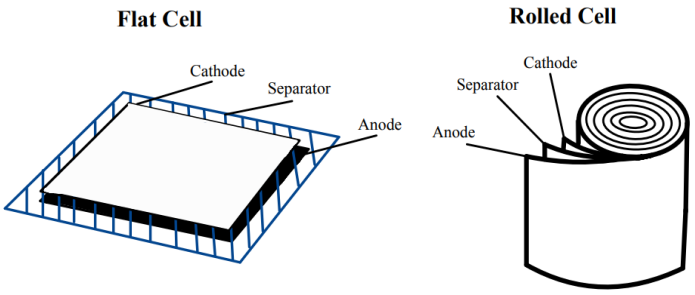

Figure 2. Flat-stacked and rolled cell configurations

3.3 List of Equations Applied to Raw Data Analysis

The formula used to calculate the standard potential of the cell is shown in Equation 1, where E^o represents the standard reduction potential of the cathode and anode. However, galvanic cells are often operated at non-standard conditions, where the Nernst Equation may be used (Equation 2). This takes into account factors such as temperature, pressure and the reaction quotient[12].

Equation 1 - Calculating the standard reduction potential of a full cell:

$$E^o = E^o\,(\text{cathode}) - E^o\,(\text{anode})$$

Equation 2 - The Nernst Equation:

$$E = E^o - \frac{RT}{nF} \ln Q$$

E^o = Reduction potential of the cell, R = Ideal gas constant (8.314 J $K^{-1}mol^{-1}$), T = Temperature (K) and n = number of electrons transferred.

Equation 3 - Ohm's Law:

Furthermore, Ohm's Law is discussed in the discussion to compare the relationship between the voltage (V), current (I) and resistance (R) within the circuit, where voltage is in volts (V), current is in amperes (A), and resistance is given in Ohms (Ω). This is rearranged as shown below to distinctly compare the current changes involving voltage and resistance.

$$V = IR$$

$$\text{This is then rearranged to: } I = \frac{V}{R}$$

The power within the cells is also studied, where power (Watts) is shown in Equation 4, with V representing the voltage (V) and I representing the Current (A).

Equation 4 - Power (W):

$$P = VI$$

To calculate the overall voltage within a series circuit, the voltage of each power source can be added, providing the final voltage as shown in Equation 5.

Equation 5 - Voltage in Series:

$$V = V_1 + V_2 + \ldots + V_n$$

4. Discussion

Our investigation compared the output and efficiency of a rolled and flat galvanic cell, as well as the effect of $ZnSO_4$ electrolyte concentration on cell output. Both cells contained a copper and zinc electrode, with a 0.1M KCl solution used as a salt bridge and separator. The standard reduction potentials for zinc and copper, as shown in Table 4, are -0.76V and 0.34V, respectively. This indicates that the copper electrode will undergo reduction, acting as the cathode. To obtain the standard potential of the cell, the reduction potential of the anode is subtracted from that of the cathode[13], as demonstrated in Equation 1. This yields an overall standard reduction potential of 1.10V for the entire cell. Table 1 shows that the voltage output for the flat stacked cell was 0.6659V, while Table 2 shows that for the rolled cell, the output was 0.7462V. This indicates a loss of 0.4341V (or an efficiency of 60.5%) for the flat stacked cell, and a loss of 0.3538V (or an efficiency of 67.84%) compared to the theoretical potential at standard conditions.

Overall, the output was much smaller than the predicted voltage output of 1.10V (Figure 4), likely due to the leakage of voltage

and current because of electrolyte leakage or unintended contact of electrodes, leading to a short circuit[14], as well as unintended contact of the electrodes due to faulty use of the separators. Additionally, another cause of shorts is the production of dendrites, which are tiny metallic projections that extend across and pierce the separator, leading to electrode contact[15].

Due to shorts and the leakage of current, differing results were observed between the rolled and flat cell batteries. For the flat cell, a voltage reading of 0.6659 V was taken, lower than the 0.7462V value taken for the rolled cell. The configuration of the cell was likely the reason for the varied data. The flat-stacked cell has great contact between the electrodes across the whole surface, facilitating the exchange of electrons, and hence leading to a greater voltage[16]. However, as seen in *Table 1*, the rolled cell can reduce the contact and uniformity of electron and ion transfer between the electrodes, leading to reduced voltage and current[17]. Furthermore, both cells had voltages significantly lower than the theoretical standard potential of 1.10 V, indicating sources of error, including the absence of a Cu^{2+} or Zn^{2+} electrolyte. Instead, a 0.1M KCl solution was used as the electrolyte, which doesn't include Cu^{2+} or Zn^{2+}, thus inhibiting the reaction as the copper cathode requires Cu^{2+} ions to be able to accept electrons and act as the reducing agent.

As shown in *Table 1*, the voltage of the circuits with no batteries was significantly lower than that of the circuits containing 2 batteries. For example, in the flat cell, the voltage with no battery was 0.6659V, while that of the rolled cell was 0.7462. This indicates that a voltage was successfully generated, despite being much lower than the predicted value of 1.10V. When 2 batteries were supplied to the circuit, the voltage of the flat cell circuit was 3.9667V while the voltage of the rolled cell circuit was 4.0321V. Adding more batteries in series directly increases the voltage because batteries themselves contain voltage, and the final voltage of the circuit is the sum of the voltage in each component of the circuit, as demonstrated in *Equation 5*. Furthermore, as a higher voltage was supplied, the current of both cells also increased (from 1.621 mA to 25.874mA in the flat cell and from 1.731mA to 26.635mA in the rolled cell), resulting from the direct proportionality of voltage and current, as demonstrated in *Equation 3*. A higher voltage provides a larger force to push a constant number of electrons through a circuit, leading to the increased current observed (Figure 3) [18].

Furthermore, *Table 2* demonstrates that in both cells, no light bulbs lit up when supplied with the voltage from only the galvanic cell; however, when the 2 batteries were added in series, all light bulbs lit up in both cells. This is because different amounts of energy are required to light up each bulb, with the red and yellow light bulbs requiring the lowest voltage to light up, at just 2 - 2.2 V. In contrast, the white, blue, and green light bulbs required the largest voltage to light up, between 3 - 3.2 V. Hence, the initial voltage of the flat and rolled cells (0.6659V and 0.7462V, respectively) didn't provide enough energy to light up the bulb, yet after adding the batteries, the voltage exceeded 3.2V in both circuits, meaning an adequate voltage was reached to light each bulb in both circuits.

Moreover, *Table 4* demonstrates that the voltage output of the Zn-Cu flat-stacked cell decreases with increasing $ZnSO_4$ concentration. Specifically, when the concentration of $ZnSO_4$ is 0.1 mol/L, the voltage is 0.958V, yet at 1.0 mol/L, this reduces to 0.8740 V, and finally, at 2.0 mol/L, the voltage drops further to 0.8505 V. The results obtained support the theoretical prediction given by the Nernst Equation (*Equation 2*), which accounts for non-standard conditions and the effect of changing ion concentrations on cell potential.

For the zinc-copper cell, the full redox reaction is:

$$Zn_{(s)} + Cu^{2+}_{(aq)} \rightarrow Zn^{2+}_{(aq)} + Cu_{(s)}$$

Under this reaction, the reaction quotient is:

$$Q = \frac{[Zn^{2+}]}{[Cu^{2+}]}$$

Assuming a constant Cu^{2+} concentration (1.0 mol/L), the Nernst Equation simplifies to a dependence on the Zn^{2+} ion concentration, which is equal to the concentration of the $ZnSO_4$ electrolyte used. Therefore, substituting this into the Nernst equation gives us:

$$E = E^{o} - \frac{RT}{nF} \ln [ZnSO_4]$$

This relationship shows that voltage decreases logarithmically as $ZnSO_4$ concentration increases, which is shown in *Figure 5*, and can be expressed in a proportional form equation as:

$$E \propto -\log[ZnSO_4]$$

This relationship reinforces the theoretical prediction that higher Zn^{2+} concentrations increase the reaction quotient (Q), therefore reducing the cell potential. A comparison between the experimentally observed voltages and the cell potentials computed using the Nernst equation is made in order to verify the theoretical model. At 298 K, the Nernst equation reduces to:

$$E = 1.10 - 0.01285 \ln[ZnSO_4]$$

E^{o} = 1.10V, R = 8.314 $JK^{-1}mol^{-1}$, T = 298 K, n = 2, F = 96,485 $C\ mol^{-1}$

Table 4 compares the theoretical voltages obtained using this equation with the observed experimental data. The observed voltages are consistently lower than the theoretical predictions derived from the Nernst equation. This disparity can be explained by several related experimental constraints and not ideal circumstances that are typical of real-world electrochemical systems. One major factor is internal resistance arising from the flat-stacked cell design. Although this configuration allows uniform surface contact between electrodes and electrolyte, resistance still arises from ionic drag in solution, imperfect electrode-wire connections, and contact resistance at the metal-clip interface[19]. These losses reduce the effective voltage when measured using the multimeter. Inconsistent placement of alligator clips on the flat electrodes also contributes to inconsistent electrical contact. Subsequently, another significant factor is the absence of Cu^{2+} ions for the cathode half-cell reaction. Theoretically, Cu^{2+} is reduced to $Cu_{(s)}$ at the cathode. However, in this experiment, only $ZnSO_4$ was used as the electrolyte, meaning that no Cu^{2+} ions were present to accept

electrons at the copper electrode. Therefore, the cathode acts as a passive conductor rather than an active reduction site, suppressing the full redox process and lowering the cell potential[20]. Finally, short circuits and measurement inconsistencies also contribute to the voltage drop. In the experimental configuration, there is a risk that the zinc and copper sheets make physical contact, bypassing the electrolyte and creating a low-resistance path. This short-circuiting can discharge the cell prematurely and skew the voltage readings[21].

The applications of rolled or flat-celled batteries are dependent on their efficiency, sustainability, and cost, regarding the specific application. The simple design of rolled cells supports automated manufacturing processes, leading to efficient production, low costs, and a high degree of uniformity.[22] The standardised manufacturing of rolled cell batteries leads to more efficient use of materials, lower energy consumption and streamlined recycling processes[23], resulting in a lower carbon footprint and a more sustainable battery configuration. Rolled cells are the cell configuration typically used in standard consumer batteries available in supermarkets. Conversely, flat-stacked cell batteries optimally use available space, enhancing energy density, making the configuration suited to applications such as smartphones and other portable electronics[24].

Overall, while the aim was fulfilled and the effects of cell type and electrolyte concentration were successfully related to the cell output (voltage and current), the investigation was invalid due to the unreliability and inaccuracy of the results acquired. Rolled cells resulted in a larger output for both the voltage and current. In circuits with no batteries, both circuits were unable to light up any of the light bulbs; however, when 2 batteries were added in series, all light bulbs were lit up in both circuits. Furthermore, a larger concentration of the electrolyte resulted in a lower voltage, as demonstrated in *Table 3*. However, the results significantly deviated from the theoretical value of 1.10V, indicating a significant source of error in our method, which would require more testing to determine the specific cause. Furthermore, due to the discrepancies between the theoretical value and the experimental value, as well as the inconsistency in results across multiple trials, our experiment is unreliable. To improve our data, more tests should be done in order to identify if the results are consistent across trials. Furthermore, testing cells which are stacked with multiple layers would have allowed conclusions to be made about the impact of surface area on the output of the cells, along with the effect of the number of layers on the ability to compact cells for storage, which could be related to the applications of cells.

5. Conclusion

Ultimately, the investigation determined that, in comparison to the flat cell, the rolled cell yielded a higher voltage and current for the same electrode surface area. For each series circuit, the voltage with no batteries was 0.6659V and 0.7462V for the flat and rolled cell, respectively. This was likely due to the uniformity of electron and ion transfer. Furthermore, increasing the concentration of the electrolyte decreased the voltage of the cell, as shown in Table 4, where the voltage of the 0.1M $ZnSO_4$ was 0.958 V compared to 0.8505 V for the 2M $ZnSO_4$. The effect of concentration is explained by the Nernst Equation (Equation2), whereby increasing the concentration of products compared to the reagents will reduce the voltage. Despite achieving the aim of the investigation, our investigation was invalid due to unreliability and significant deviations from the theoretical values. To improve our investigation, the number of trials should be increased to test for consistency, and the surface area should be increased by stacking more electrodes to investigate the effect of surface area on electron transfer and power density. Irrespective, future research could explore the use of sustainable or biodegradable electrode and electrolyte materials to minimise the environmental impact of galvanic cells, making electrochemical cells more viable for green energy storage solutions[25]. Additionally, optimising cell geometry and reducing internal resistance could contribute to the development of more efficient, compact energy systems for both portable electronics and renewable energy applications.

Authorship Contribution Statement

Emily Sewell co-wrote the abstract, introduction, discussion, and conclusion, wrote the materials & methods and contributed to the discussion. Manas Srinivas co-wrote the abstract, introduction, materials & methods, discussion, conclusion, and conducted the literature review. Lucas Sidney compiled the data tables and processed experimental results. Jacinta Wilkin contributed to drafting the discussion, reviewed and edited the full manuscript, and contributed to the final referencing. Bryan Law analysed trends in voltage and electrolyte concentration and wrote the equations and derivations. Dr. Thomas Whittle designed the experiment. Dr. David Alam facilitated project resources and guidance on conceptual direction. Dr. Gobinath Rajarathnam ideated conceptual direction, research and writing guiding frameworks, and direct project supervision.

Acknowledgements

Along with the use of generative AI, Group 7's (Madison Louey, Melissa Marshall, Jun Wei Wong, Audrey Wang, Alan Lun) raw current and voltage data, compared to the concentration of $ZnSO_4$, as seen in Table 3, were incorporated to determine and evaluate the effect of concentration on voltage.

References

1. Jeon, B.-J., Lee, Y.-H. & Jeong, K.-M. Unveiling the Impact of Electrode Curvature on N/P Ratio Variations in Cylindrical Lithium-ion Batteries. *Energy storage materials* 104117–104117 (2025) doi:https://doi.org/10.1016/j.ensm.2025.104117.

2. Janzen, A. F. Photoelectrochemistry II - The Photogalvanic Cell *Elsevier eBooks* 923–937 (1979) doi:https://doi.org/10.1016/b978-0-08-024744-1.50036-x.
Bhattacharjya, D., Carriazo, D., Ajuria, J. & Villaverde, A. Study of electrode processing and cell assembly for the optimised performance of supercapacitor in pouch cell configuration. *Journal of Power Sources* 439, 227106 (2019).

3. Zhu, J. *et al.* End-of-life or second-life options for retired electric vehicle batteries. *Cell Reports Physical Science* 2, 100537–100537 (2021).

4. Saber, N., Richter, C. P. & Runar Unnthorsson. Review of Thermal Management Techniques for Prismatic Li-Ion Batteries. *Energies* 18, 492–492 (2025).

5. Electrochemistry: Galvanic Cells and the Nernst Equation. *Chemcollective.org* https://chemcollective.org/chem/electrochem/step2_cell.php#:~:text=In%20the%20movie%20on%20the,Tap%20to%20unmute (2021).

6. Nazarian-Samani, M., Alidokht, S. A., Heloise Therien-Aubin & Zhang, L. Mechanical structure design: A survey on modern triboelectric nanogenerators. *Applied Energy* 391, 125918–125918 (2025).

7. Moradi, H. G., Mahdavi, M. A., Reza Gheshlaghi & Mozhdeh Dehghanian. Electrochemical evaluation of the effect of anode to cathode surface area ratio on power generation in air-cathode microbial fuel cells. Journal of Applied Electrochemistry 53, 2433–2442 (2023).

8. JEI. Analysis of reduction potentials to determine the most efficient metals for electrochemical cell alternatives | Journal of Emerging Investigators. Emerginginvestigators.org https://emerginginvestigators.org/articles/19-088 (2020).

9. Yang, N. *et al.* Magnesium galvanic cells produce hydrogen and modulate the tumour microenvironment to inhibit cancer growth. *Nature Communications* 13, (2022).

10. Alberts, B. *et al.* The Mitochondrion. *Nih.gov* https://www.ncbi.nlm.nih.gov/books/NBK26894/#:~:text=The%20electrochemical%20proton%20gradient%20across,enzyme%20ATP%20synthase%2C%20mentioned%20previously. (2025).

11. Feiner, A.-S. & McEvoy, A. J. The Nernst Equation. Journal of Chemical Education 71, 493 (1994).

12. Waag, W. & Sauer, D. U. SECONDARY BATTERIES – LEAD–ACID SYSTEMS | State-of-Charge/Health. Elsevier eBooks 793–804 (2009) doi:https://doi.org/10.1016/b978-044452745-5.00149-0.

13. Shea, H. R. et al. Effects of Electrical Leakage Currents on MEMS Reliability and Performance. IEEE Transactions on Device and Materials Reliability 4, 198–207 (2004).

14. Peng, J. et al. Electrolyte effects on the electrochemical performance of microemulsions. Electrochimica Acta 393, 139048–139048 (2021).

15. Timurkutluk, B., Timurkutluk, C., Mat, M. D. & Kaplan, Y. A review on cell/stack designs for high-performance solid oxide fuel cells. Renewable and Sustainable Energy Reviews 56, 1101–1121 (2016).

16. Willert, A., Voigt, S., Zschau, T. & Zichner, R. Printed Primary Battery in a Rolled-Up Form Factor. Designs 8, 62 (2024).

17. Licari, J. J. & Swanson, D. W. Functions and theory of adhesives. Elsevier eBooks 35–74 (2011) doi:https://doi.org/10.1016/b978-1-4377-7889-2.10002-6.

18. Moral, C. G. et al. Battery Internal Resistance Estimation Using a Battery Balancing System Based on Switched Capacitors. IEEE Transactions on Industry Applications 56, 5363–5374 (2020).

19. Zavalis, T. G., Behm, M. & Lindbergh, G. Investigation of Short-Circuit Scenarios in a Lithium-Ion Battery Cell. Journal of The Electrochemical Society 159, A848–A859 (201).

20. Zavalis, T. G., Behm, M. & Lindbergh, G. Investigation of Short-Circuit Scenarios in a Lithium-Ion Battery Cell. *Journal of The Electrochemical Society* 159, A848–A859 (2012).

21. Schröder, R., Aydemir, M. & Seliger, G. Comparatively Assessing different Shapes of Lithium-ion Battery Cells. Procedia Manufacturing 8, 104–111 (2017).

22. Wilke, C., Kaas, A. & Urs Alexander Peuker. Influence of the Cell Type on the Physical Processes of the Mechanical Recycling of Automotive Lithium-Ion Batteries. Metals 13, 1901–1901 (2023).

23. Sabri Baazouzi et al. Design, Properties, and Manufacturing of Cylindrical Li-Ion Battery Cells—A Generic Overview. Batteries 9, 309–309 (2023).

24. Ayat Gharehghani et al. Progress in battery thermal management systems technologies for electric vehicles. Renewable and Sustainable Energy Reviews 202, 114654–114654 (2024).

Appendix

Table 1. Raw data reflecting the flat-stacked and rolled cell voltage, current, and power, with one battery and two batteries.

Battery Type	Voltage (V)		Current (mA)		Power (mW)	
	No Battery	With 2 Batteries	No Battery	With 2 Batteries	No Battery	With 2 Batteries
Flat-stacked battery cell	0.6659	3.9667	1.621	25.874	1.079	102.7
Rolled battery cell	0.7462	4.0321	1.731	26.635	1.2917	107.39

Table 2. Raw data reflecting LED colour, corresponding wavelength, required voltage and light-up test.

Flat-Stacked and Rolled Battery Layout	LED Colour	Wavelength (nm)	Required Voltage (V)	Activated
No Battery	Red	625-750	2.0 - 2.2	No
	Yellow	565-590		
	White	400-700	3.0 - 3.2	
	Blue	450-485		
	Green	500-565		
2 Batteries	Red	625-750	2.0 - 2.2	Yes
	Yellow	565-590		
	White	400-700	3.0 - 3.2	
	Blue	450-485		
	Green	500-565		

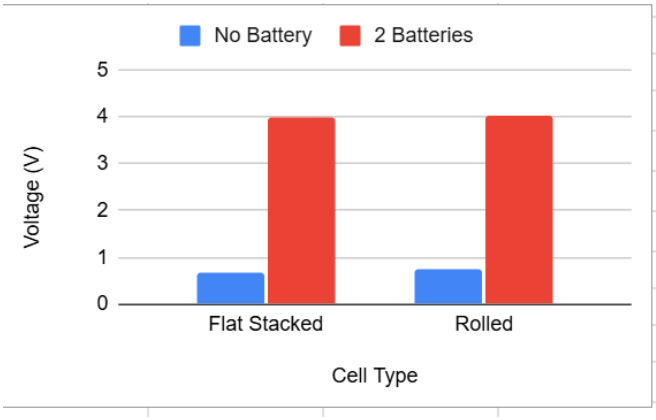

Figure 3 - The voltage in a flat cell and a rolled cell with no battery compared to 2 batteries.

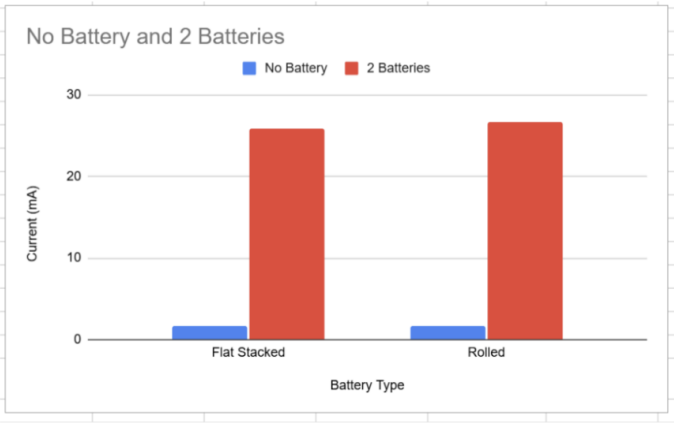

Figure 4 - The current in a flat cell and a rolled cell with a battery compared to 2 batteries.

Table 3. Raw data reflecting changes in the voltage, current and power compared to the concentration of $ZnSO_4$

Concentration of $ZnSO_4$ (mol/L)	Voltage (V)	Current (mA)	Power (mW)
0.1	0.958	25.874	24.787
1	0.874	23.724	20.735
2	0.8505	22.851	19.435

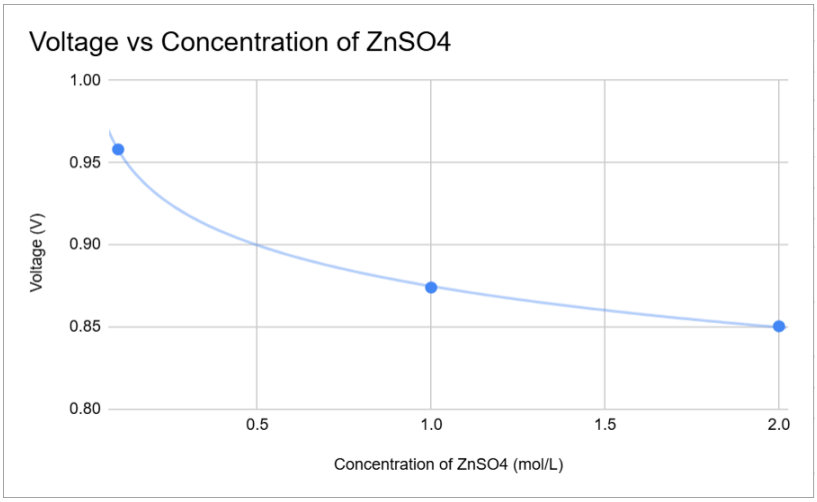

Figure 5 - The concentration of $ZnSO_4$ electrolyte compared to the voltage produced

Table 4. The difference between the theoretical voltage and experimental voltage at different $ZnSO_4$ concentrations

$ZnSO_4$ (mol/L)	ln[$ZnSO_4$]	Theoretical Voltage (V)	Observed Voltage (V)	% Difference
0.1	-2.3026	1.1296	0.9580	15.2%
1.0	0.0000	1.1000	0.8740	20.5%
2.0	0.6931	1.0911	0.8505	22.0%

The Sydney Journal of Interdisciplinary Engineering
SJIE 1(1) X–X (2025) https://doi.org/XXXX/XXXX

Analysing the impact of Potassium Chloride Concentration on the Electrical behaviour of a Rolled Galvanic cell

Ryan Ng, Noah Evans, Julian Bray, Alana Mansfield, Kuanxin Liu, Jordan Kambanis, Masoomeh Ashgar Nejad-Laskoukalayeh, Benedict Tai, David Alam, Thomas Whittle, Gobinath Rajarathnam

E-mail: ryng0870@uni.sydney.edu.au

Abstract

This study explores how the concentration of the salt bridge electrolyte affects the performance of a rolled Zn–Cu galvanic cell. By using KCl at two concentrations of 0.1 M and 0.5 M, we observed that increased electrolyte concentration resulted with an 8.4% increase in power output. Voltage rose from 0.7669 V to 0.7839 V, current from 2.202 mA to 2.335 mA, and internal resistance decreased from 0.348 Ω to 0.336 Ω. Although the salt bridge does not participate directly in redox reactions, our findings highlight its significant role in charge transport. These results suggest that optimizing electrolyte concentration offers a simple yet effective strategy to improve cell efficiency without altering core components of the cell such as electrode material. This has implications to optimise energy use within rural regions or disaster zones. Further research should explore a broader range of concentrations and electrolyte types, with statistical validation and time-based performance analysis.

Keywords: zinc–copper battery, salt bridge, electrolyte concentration, power output

1. Introduction

A battery is a device that converts chemical energy into electrical energy through a series of redox (reduction and oxidation) reactions. The system which defines the battery is also known as an electrochemical cell[1]. It consists of both an anode and cathode, where oxidation and reduction occur respectively. In a classic galvanic cell, the electrodes are immersed in an electrolyte, which facilitates the migration of ions which is necessary to sustain the redox reactions and maintain charge neutrality[2], otherwise resulting in an imbalance of positive and negative charges. As oxidation at the anode releases electrons, these electrons travel through an external circuit toward the cathode, where they are consumed in the reduction reaction[3]. The resulting flow of electrons constitutes an electric current (DC), which can power an external load. Simultaneously, the internal movement of ions within the electrolyte completes the circuit, ensuring the ongoing operation of the cell. This complementary transport of electrons and ions is fundamental to the function of all battery systems[4].

Recently, there have been many studies which have addressed the simple, copper zinc galvanic cell due to its relatively cheap cost. A study performed by Mohammad Ali Amayreh focused on developing a low-cost, small-scale Zn-Cu galvanic cell using common materials like galvanized nails and copper wires, demonstrating that even with diluted electrolytes, the cell could generate usable voltage[5]. Meanwhile, a separate study explored the potential of

rechargeable Zn-Cu batteries by introducing a cation exchange membrane to prevent copper ion crossover, a major limitation in traditional Daniell cells[26]. These innovations highlight a growing interest in sustainable and scalable battery designs using abundant materials like zinc and copper. It was found that salt concentration increasing in diluted electrolytes was found to enhance ion transport within cells7. However, these study's often focus either on large scale applications or on traditional cell geometries[8]. There remain limited experimentations of how experimenting with the ionic conductivity of a salt bridge effects the overall cell, in regard to a low cost, rolled cell[9]. While cell stacking has been examined in relation to the output in flat cells, this study focuses on the rolled configuration due to its simplicity[10]. Batteries are essential in applications ranging from household electronics to transportation and medical devices11. Zinc–copper cells offer a low-cost, non-toxic option for powering small-scale systems such as remote sensors and educational devices. Their ability to deliver efficient DC output makes them ideal for portable, low-power applications[12].

The aim of this experiment is to assess the performance of a "rolled cell" configuration by systematically varying the electrolyte concentration. Through this investigation, we seek to determine whether changes in electrolyte concentration significantly impact the electrical output of the rolled cell, providing insight into the role ionic conductivity can play in energy output.

2. Methods

2.1 Cell Construction

To construct the rolled battery, 8cm by 4cm sheets were cut out of the Copper and Zinc foil, and were compared to ensure identical shape and form. The electrolyte was diluted in the glass measuring cylinder with distilled water to determine the concentration of the electrolyte. Following the dilution of the electrolyte, two sheets of filter paper were cut to the same 8cm by 4cm dimensions of the electrodes and were set aside. Approximately ~10ml of the electrolyte was decanted into the petri dish, and the first strip of filter paper was soaked in the electrolyte until fully saturated. This filter paper soaked in electrolyte acts as both the salt bridge for the battery, ensuring electrical neutrality and a separator which inhibits the anode and cathode from touching and short circuiting. The soaked filter paper was placed in between the copper and zinc strips, and the second strip of filter paper was soaked and laid upon the stack. The total arrangement of layers being copper, separator, zinc, separator. Once constructed, the sheets were rolled into a cylindrical shape, and taped so that they wouldn't unwind, great care was taken to ensure no contact between electrodes, but also no overlap in spacer material, as this could lead to mechanical failure.

Once constructed, the positive lead of the multimeter was attached to the copper sheet, and the negative lead to the zinc sheet (Figure 1).

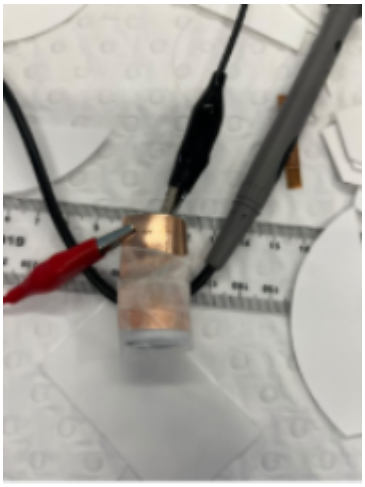

Figure 1: *Rolled cell. Soaked filter paper placed in between the copper and zinc strips, and with a second strip of filter paper was soaked and laid upon the stack. The sheets are rolled into a cylindrical shape, and taped to prevent unwinding. The positive lead of the multimeter is attached to the copper sheet, and the negative lead to the zinc sheet.*

2.2 Equipment and materials

Table 1*: List of equipment and materials used for the construction and testing of the rolled Zn–Cu galvanic cell, including measurement tools and electrolyte components.*

Copper Foil Sheet	Multimeter (UNI-T UT181A)
Zinc Foil Sheet	Alligator Clips and Wires
Filter Paper	LED lights (varied colours)
0.1M Copper (III) Sulfate solution ($CuSO_4$)	Scissors
0.1M Zinc Sulfate solution ($ZnSO_4$)	Tape
0.1M Potassium Chloride solution (KCl)	Ruler
Distilled Water	Glass Measuring Cylinder
Plastic Petri Dishes	Beakers
Metal Tweezers	

2.3 Data collection

Measurements of voltage and current were collected from rolled Zn–Cu galvanic cells constructed as described in Section 2.1. Each cell was tested under two experimental conditions: 0.1 M and 0.5 M KCl as the supporting electrolyte. The cell was allowed to rest for around 30 seconds before testing. For each cell, voltage was tested before the current of the cell, as to not draw current.

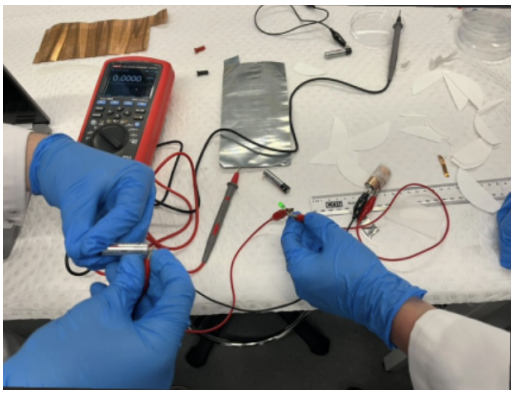

Figure 2: *Rolled Zn–Cu galvanic cell setup using KCl-soaked filter paper as a salt bridge and separator. The cell is connected to a UNI-T UT181A multimeter via alligator clips and wires, with a green LED light used to indicate current flow.*

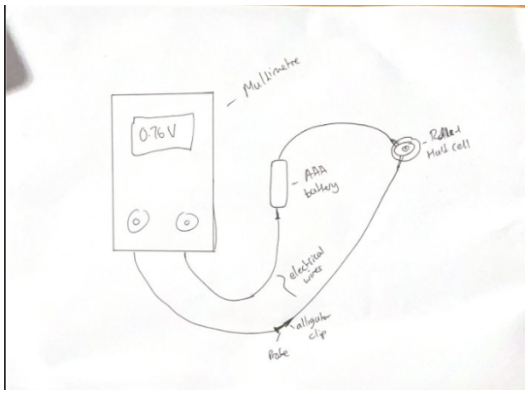

Figure 3: *Diagram of experimental setup including the multimeter, rolled cell, battery and connecting wires.*

3. Results

Results. In this study we examined how changing concentrations of the salt bridge effects the performance of a Zn – Cu rolled cell. The performance of the Zn–Cu rolled galvanic cell was assessed under two different potassium chloride (KCl) concentrations: 0.1 M and 0.5 M. Increasing the concentration of the KCl electrolyte resulted in a modest increase in both voltage and current. At 0.1 M, the average voltage recorded was 766.9 mV and the current was 2.202 mA. At 0.5 M, the voltage rose to 783.9 mV and the current to 2.335 mA, corresponding to approximate increases of 2.2% and 6%, respectively (Table 2).

3.1 Data analysis

The following formulas were used to calculate Power, resistance for calculations.

Power: =

where V and I represent Voltage and current, respectively.

Specific power = P/A(electrode)

where electrode area = 0.03 x 0.06 = 0.0018m

Resistance: =

Data trends were visualised using line plots of KCl concentration versus voltage, current, and power output.

Table 2: *Voltage and current at each KCL concentration. Measured open-circuit voltage and current output of the Zn–Cu rolled galvanic cell at two potassium chloride (KCl) concentrations (0.1 M and 0.5 M).*

CONC of KCL	**Current (mA)**	**Voltage (mV)**
.1M	2.202	0.7669
.5M	2.335	0.7839

These measurements were used to derive additional performance metrics, including power, internal resistance, and specific power. Power output increased from 1.689 mW to 1.830 mW — an 8.4% improvement — while internal resistance decreased from 0.348 Ω to 0.336 Ω. Specific power, defined relative to electrode surface area, also rose from 938.17 to 1016.89 mW/m² (Table 3).

Table 3: *Derived electrical characteristics of the Zn–Cu rolled galvanic cell at two KCl concentrations. Power, resistance, and specific power were calculated based on measured voltage and current values*

CONC of KCL	Power	Efficiency	Resistance	Specific Power:
.1M	1.689	0.697	0.348	938.17
.5M	1.830	0.713	0.336	1016.89

Trends across both current and voltage showed a slight linear increase with higher KCl concentrations (Figure 3), which contributed to the observed increase in power output (Figure 4). These results suggest that enhanced ionic conductivity in the salt bridge, driven by greater electrolyte concentration, plays a meaningful role in improving charge transport within the cell. However, given the limited range and number of data points, further testing would be needed to confirm whether this relationship is consistently linear or follows another pattern.

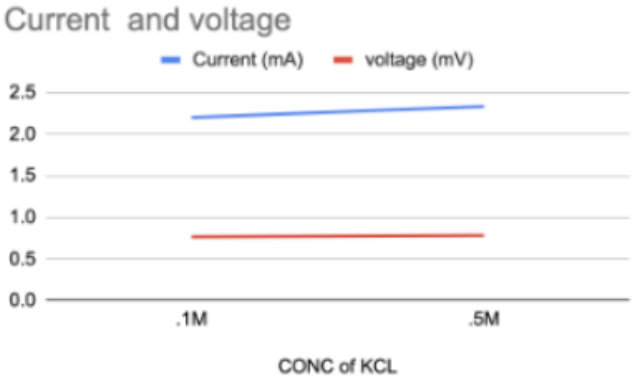

Figure 4: Current (blue, mA) and voltage (red, mV) output of a Zn–Cu rolled galvanic cell at two different KCl concentrations (0.1 M and 0.5 M). A slight increase in both parameters is observed with increased KCl concentration.

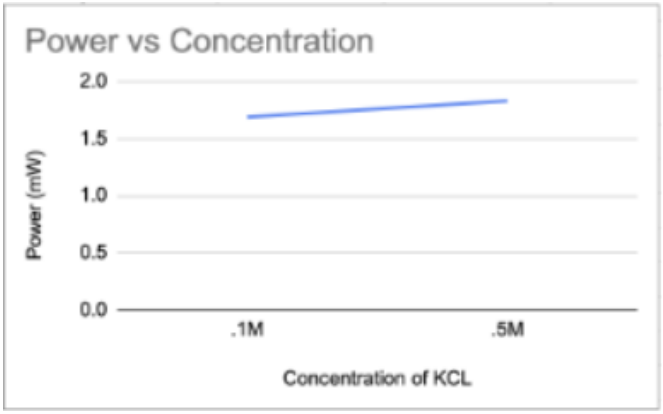

Figure 5: Power output (mW) of a Zn–Cu rolled galvanic cell as a function of potassium chloride (KCl) concentration (0.1M, 0.5M) in the electrolyte-soaked salt bridge

4. Discussion

4.1 interpretation of results and theoretical explanation

Redox half equations:

$$Zn_{(s)} \rightleftharpoons Zn^{2+}_{(aq)} + 2e^- \qquad \text{-0.76V (reduction)}$$

$$Cu^{2+}_{(aq)} + 2e^- \rightleftharpoons Cu_{(s)} \qquad \text{+0.34V (oxidation)}$$

$$Cu^{2+}_{(aq)} + Zn_{(s)} \rightleftharpoons Cu_{(s)} + Zn^{2+}_{(aq)} \quad \text{+1.10V}$$

The standard potential of the cell $E°$ in the Nernst Equation) is calculated by subtracting the reduction from the oxidation or the anode from the cathode which as an equation is represented as

$$E^{\circ}_{(cell)} \; E^{\circ}_{(cathode)} E^{\circ}_{(anode)}$$

For this specific redox reaction, the standard potential of the cell or $E^{\circ}_{(cell)}$ is 1.10V.

With limited results no valid and reliable judgments can be made however based on the trends from the limited data increasing the concentration of electrolyte increasing both the current and the voltage produced by the half cell with the voltage and current at a KCl concentration of 0.1M being 0.7669V and 2.202A respectively, constituting slightly lower values then the ones produced by a solution of 0.5M KCl with the voltage produced being 0.7839V and the current being 2.335A. Unfortunately, this does not provide evidence for either a non-linear or linear trends. Based off theoretical results from several published papers, the gathered experimental results do not follow typical Nernstian behaviour with Nernstien's equation proposing that an increase in the electrolyte concentration should decrease the cell potential and thus the voltage[13]. This suggests that the electrolyte does not directly participate in the redox reactions of the half cell and instead only facilitates the flow of ions which is why increasing the concentration increases the voltage[14].

4.2 Comparison to Literature

A review of recent literature suggests that battery performance is not both a function of electrolyte concentration

but also strongly affected by the cell's architecture and electrode design[15]. For instance, studies have shown that modified electrode structures such as those employing 3D porous materials or increased effective surface area can improve ion transport and promote a more uniform deposition of metal ions, thereby reducing the risk of dendrite formation[16]. As noted before, while electrolyte concentration does not universally affect ion mobility in every circumstance[17], it's important to note in the context of our experiment it is the most likely cause. A recent study on flat, paper-based Zn–Cu cells demonstrated that stacking enhances voltage and stability by increasing surface are[18]. Although not focused on rolled cells, the rolled configuration may achieve similar performance gains via increased interfacial area per unit volume.

Given we have attempted to control size, shape and temperature of the electrode, our independent variable was our concentration. As the concentration increased, the observed improvement in performance suggests enhanced ionic conductivity was likely due to improved ion mobility within the salt bridge, which facilitates more efficient charge transport between electrodes[19].

4.3 Real world implications

Although this study was limited in scope due to a limited examination of the effect of concentration of electrolyte had on the performance of a rolled cell, the findings have a broader implication outside of this context. It implies the importance of optimising ionic conductivity to improve the outputs of galvanic cells[20]. This highlights how minor improvements to how a battery is constructed can have noticeable changes in energy delivery. On a larger industrial scale, this could lead to quantifiable gains in energy delivery, increasing the more efficient use of resources[21].

A zinc copper rolled galvanic cell is the definition of simplicity. As such, the results are relevant in scenarios where cost and simplicity are prioritised[22]. Single-use detectors such as environmental monitors often rely on minimalistic battery designs, where opportunities for electrical optimisation such as reducing internal resistance are limited due to size and cost[23]. Low cost and effective adjustments to the salt bridge which can boost performance are often required.

In a boarder scope, it suggests the feasibility of using low toxic systems such as Zn – Cu galvanic cells in portable energy systems[24]. Such an application is often overlooked in conventional battery research, given the increasing need to power to operate, however, to provide this requires materials which are accessible but also operate at cost efficiency. Being able to optimise a low costs system is helpful, especially if used in application such as energy kits for schools, rural communities or in disaster zone. This could include LED lanterns, water quality assessors, and devices which operate under low current loads and doe does not require a complex recharging infrastructure[25].

4.4 Limitations

While the experimental outcomes provided insight into how electrolyte concentration effected the performance of a galvanic cell, many factors restrict the interpretability and generalisation of our results. The study was limited to two, non-repeated concentrations of KCL (0.1M, 0.5M) which restricts the extrapolation of the graph beyond the two given points. It provides no indication of outliers within the dataset due to the absence of either a linear or non-linear trend. This was also due to no repetitions at each concentration, resulting in the inability to perform any statistical measures to mitigate the effects of potential outliers. This absence of repetition also introduces uncertainty surrounding replication of produced results, which is very important if used for research purpose. Variation of Seperator absorption of electrolyte, inconsistencies of material surface and tightness of roll could all effect performance, especially at mV and mA scales, where small alterations can result in significant percentage deviations26. This study was also limited to one type of electrolyte, as we did not explore different electrolyte types.

Furthermore, during experimental preparation, many issues arose due to time constraints and a lack of underlying knowledge before beginning the experiment. This led to a large portion of the allocated time being spent experimenting with getting a working cell battery having many failed attempts due to things such as touching anode and cathode as well as incorrect placement of the voltmeter cables, breaking the circuit. Ultimately, this caused our results to be incomplete, only being able to measure the voltage and current caused by the 0.5M and 0.1M solutions of KCl compared to our intended goal of measuring voltage and current for 0.1, 0.2, 0.3, 0.4 and 0.5 molar concentrations of KCl which would have given us a better range and a deeper understanding of how the electrolyte concentration can affect the voltage and current of a rolled half-cell.

4.5 Future improvements and consideration

To solve this, having both more gradual increments between concentration and more concentrations would be necessary to determine whether the exists an optimal concentration beyond or between 0.5M, and what sort of overall trend we can observe. Future studies should also include replicate trials for each condition to assess the variability between each build of battery.

Future research should focus on expanding the range of electrolytes tested and investigating the performance of the cell over continuous and repeated usages. Additionally, it may be important to investigate varying cell geometries such as stacked and flat cells. This modification will enhance our understanding of how simple modifications can enhance galvanic cell performance for applied contexts.

5. Conclusion

This study addresses how varying concentrations of KCl of a copper zinc rolled cell effects its electrical performance. We noted that an increase in concentration from 0.1M to 0.5M correlated to a noticeable increase in power output (8%), with a marginal decrease in resistance and increase in both voltage and current. Although we had a limited set of data, this indicated that increasing the concentration plays a noticeable role in ion transport, thus affecting current of the cell more than the voltage.

These findings have broader implications. It captures the importance of electrolyte optimisation as a method of improving cell performance; one which is both low cost and low in complexity. It does not require changing of core components of a battery, and thus, such a method for cell optimisation can be applied in contexts where both simplicity and cost are important factors.

However, this study's scope was limited by lack of tested concentrations and lack of testing over time period. This study failed to gauge trends between concentration and its outputs. These limitations suggest that future work should expand the range and granularity of electrolyte concentrations, investigate alternative salts, and include long-term performance assessments to evaluate time-based stability. Repeated trials and statistical analysis will be essential to validate trends and ensure reproducibility.

This work captures the potential for small, but impactful changes to cell design, such as salt bridge optimisation, to allows cells to be more cost effective yet effective in relevant fields.

Acknowledgements

This report was primarily written by Ryan Ng who did the intro, most of the results and the references while also making major contributions to the discussion and the editing of the document. Noah Evans and Julian also put in substantial contributions with Noah making major contributions to the discussion the acknowledgements and editing and Julian being the substantial contribtor in the completion of the methods system. Alana Mansfield also made significant contributions relating to editing and formattng as well as minor contributions to proofreading and the method. Kuanxin Liu, made very minor contributions to the article. Furthermore, acknowledgements are extended to Dr. Gobinath Rajarathnam as well as Jordan Kambanis, Masoomeh Ashgar Nejad-Laskoukalayeh, Benedict Tai, Dr David Alam, Dr Thomas Whittle for their significant contributions in overseeing the experiment as well as providing us with the necessary resources to write the article. Furthermore, the creation of this report would not be possible without the University of Sydney who provided the site and equipment for which all practical experimentation was completed.

References

[1] How a battery works. Australian Academy of Science https://www.science.org.au/curious/technology-future/batteries (2016).

[2] Loayza, J. M. Allen J. Bard, Larry R. Faulkner. www.academia.edu.

[3] Solubility of Things. Applications of Galvanic Cells | Solubility of Things. Solubilityofthings.com https://www.solubilityofthings.com/applications-galvanic-cells (2025).

[4] Chen, Y. et al. A review of lithium-ion battery safety concerns: The issues, strategies, and testing standards. Journal of Energy Chemistry 59, 83–99 (2021).

[5] Amayreh,M. Low-cost, Environmentally Friendly Galvanic Cells. https://theaic.org/pub_thechemist_journals/Vol-93-No-1/Vol-93-No1-article-6.pdf (2022).

[6] Jameson, A., Khazaeli, A. & Barz, D. P. J. A rechargeable zinc copper battery using a selective cation exchange membrane. Journal of Power Sources 453, 227873 (2020).

[7] Lea Sophie Kremer et al. Influence of the Electrolyte Salt Concentration on the Rate Capability of Ultra-Thick NCM 622 Electrodes. Batteries & supercaps 3, 1172–1182 (2020).

[8] Pegel, H., Wycisk, D. & Sauer, D. U. Influence of cell dimensions and housing material on the energy density and fast-charging performance of tabless cylindrical lithium-ion cells. Energy Storage Materials 60, 102796 (2023).

[9] Giffin, G. A. The role of concentration in electrolyte solutions for non-aqueous lithium-based batteries. Nature Communications 13, 5250 (2022).

[10] Zhang, X. et al. Zinc-based fiber-shaped rechargeable batteries: Insights into structures, electrodes, and electrolytes. Nano Research (2024) doi:https://doi.org/10.26599/nr.2025.94907025.

[11] Rawat, S. et al. Advancements in Specialty Batteries: Innovations, Challenges, and Future Directions. Journal of Alloys and Compounds 179387–179387 (2025) doi:https://doi.org/10.1016/j.jallcom.2025.179387.

[12] BREY, J. et al. Power conditioning of fuel cell systems in portable applications. International Journal of Hydrogen Energy 32, 1559–1566 (2007).

[13] Li, B. et al. Challenges and opportunities facing zinc anodes for aqueous zinc-ion battery. Energy Materials and Devices 2, 9370044 (2024).

[14] Lockett, V., Horne, M., Sedev, R., Rodopoulos, T. & Ralston, J. Differential capacitance of the double layer at the electrode/ionic liquids interface. Physical Chemistry Chemical Physics 12, 12499 (2010).

[15] 15.

[16] Moraes, C. V. & Kelly, R. G. A comparison of FEM results from the use of different governing equations in a galvanic cell part II: Impact of low supporting electrolyte concentration. Electrochimica Acta 468, 143153 (2023).

[17] Ishengoma, F. R. A Novel Design of IEEE 802.15.4 and Solar Based Autonomous Water Quality Monitoring Prototype using ECHERP. arXiv.org https://arxiv.org/abs/1410.1773 _____ (2025).

[18] Zhu, P., Slater, P. R. & Kendrick, E. Insights into architecture, design and manufacture of electrodes for Lithium-ion batteries. Materials & Design 111208 (2022) doi:https://doi.org/10.1016/j.matdes.2022.111208.

[19] Zhou, L.-F. et al. Interface engineering for functionalized ultra-thin zinc anodes in aqueous zinc-ion batteries. Cell Reports Physical Science 6, 102565 (2025).

[20] Rajesh, A. Effect of Electrolyte Concentration on the Efficiency of Electrochemical Cells in India. Journal of Chemistry 3, 31–41 (2024).

[21] Hu, F., Fang, X. X., Yue, C. & Yang, Y. Three-Dimensional Architectures for Silicon Wafer-Based Integrated Microenergy Storage Systems. Small (2025) doi:https://doi.org/10.1002/smll.202412301.

[22] Chen, F. et al. Multiscale simulation and AI techniques for optimizing electrolyte injection processes. Cell Reports Physical Science 102463–102463 (2025) doi:https://doi.org/10.1016/j.xcrp.2025.102463.

[23] Golberg, A., Rabinowitch, H. D. & Rubinsky, B. Zn/Cu-vegetative batteries, bioelectrical characterizations, and primary cost analyses. Journal of Renewable and Sustainable Energy 2, 033103 (2010).

[24] Frenck, L., Sethi, G. K., Maslyn, J. A. & Balsara, N. P. Factors That Control the Formation of Dendrites and Other Morphologies on Lithium Metal Anodes. Frontiers in Energy Research 7, (2019).

[25] Lacina, K., Sopoušek, J., Skládal, P. & Vanýsek, P. Boosting of the output voltage of a galvanic cell. Electrochimica Acta 282, 331–335 (2018).

[26] NSSN. Project aims to replace sensors' toxic batteries with a greener solution. NSSN https://www.nssn.org.au/news/2024/9/9/tg5bbgpinaxq2133k2hp2srm35usbr (2024).

[27] WinAck. The consistency of battery cells is important for power battery pack. Winackbattery.com https://www.winackbattery.com/news/consistency-of-power-battery-cells.html (2015).

SJIE 1(1) X–X (2025) https://doi.org/XXXX/XXXX

Electrolyte concentration effects on Zn-Cu galvanic cells: Powering LEDs through redox optimisation

Anastasiia Danshyna [a], Grace Mihaljevic [a], Stefano Furlan [a], Isaac Sleath [a], Alexander Palmer [a], Jordan Kambanis [a], Masoomeh Asghar Nejad-Laskoukalayeh [a], Benedict Tai [a], David Alam [a], Thomas A Whittle [a], Gobinath Rajarathnam [a].

[a] *School of Chemical and Biomolecular Engineering, The University of Sydney, Sydney, NSW, 2006, Australia*

ARTICLE INFORMATION

Keywords: Battery, Electrochemistry Energy Storage, Galvanic Cell, Redox Reactions

ABSTRACT

This study investigated the effect of electrolyte concentration on the performance of Zn-Cu galvanic cells and their ability to power LEDs with different voltage requirements. Three half-cells were constructed using Zn and Cu electrodes, each immersed in electrolyte solutions of different molarities. Each configuration was tested individually and in series to assess voltage output and LED activation. Results showed that higher molarity solutions produced slightly higher voltages, and connecting cells in series increased total voltage. While single cells could not power any LEDs, series connections of two and three cells successfully powered low- and high-threshold LEDs, respectively. These findings highlight key redox and electrochemical principles relevant to practical energy applications. Electrochemical systems based on similar reactions are essential in medical implants, electric vehicles, and next-generation energy storage technologies, where efficient and reliable power delivery is at the heart of these applications.

1.Introduction

Electrochemical systems based on aqueous zinc (Zn) chemistry have gained renewed attention due to their inherent safety, material abundance, low toxicity, and adaptability to diverse cell configurations [1]-[3]. Among these, the classical zinc-copper (Zn-Cu) galvanic cell remains one of the most recognisable and instructive configurations in both pedagogical and exploratory electrochemistry. Originally conceptualised in the early 19th century, this system played a foundational role in shaping the understanding of redox processes and battery operation [4]. Today, while its role as a commercial power source has diminished, the Zn-Cu cell continues to offer significant value for educational experimentation, laboratory-scale power generation, and as a benchmark system for understanding the influence of electrolyte and cell design variables on electrochemical performance [5].

The operation of the Zn-Cu cell is governed by the redox couple Zn^{2+}/Zn at the anode and Cu^{2+}/Cu at the cathode, producing a theoretical open-circuit voltage in the range of 0.5 to 1.5 V direct current (dc) under standard conditions [6]. While the basic electrochemical pathway has remained unchanged for over two centuries, advances in electrode materials, separator technologies, and electrolyte formulation have improved the understanding of how to modulate and optimise galvanic-cell behaviour [7]. These improvements are particularly relevant as simple redox pairs re-emerge in next-generation aqueous systems such as zinc-bromine flow batteries and hybrid zinc-ion devices [8].

Historically, the Daniell cell -an archetypal Zn-Cu configuration introduced in 1836- addressed earlier limitations of hydrogen evolution and electrode passivation by employing separate electrolyte compartments and a porous barrier [4]. This conceptual separation of ionic environments remains critical in contemporary flow-battery and hybrid electrochemical systems.

The electrolyte concentration plays a dual role: it directly influences the cell potential via the Nernst equation and indirectly governs the ionic conductivity and mass transport [9]. This paper focuses on quantifying how variations in zinc sulphate ($ZnSO_4$) and copper sulphate ($CuSO_4$), molarity affects open-circuit voltage, discharge power, and light-emitting diodes (LED)-driving capability with the series wiring topology, which is commonly used in electrical engineering practices in battery cell connections.

The aim of this paper is to systematically evaluate the impact of electrolyte concentration and cell configuration on the performance of laboratory-scale Zn-Cu galvanic cells.

The objectives are twofold; firstly, to quantify the relationship between electrolyte molarity (0.5-1.5 mol/L) and dc voltage, current, and power output. The second goal is to compare three practical cell-stack configurations with series-

only electrical connection, in their ability to power small devices such as LEDs.

The remainder of this paper is organised as follows: Section 2 describes the materials, concentrations, and electrical configurations tested. Section 3 presents the experimental results, including voltage, current and power parameters with LED forward dc voltage activation thresholds. Section 4 discusses the implications of these results in the context of galvanic-cell optimisation and redox-battery design in the context of chemical engineering. Section 5 offers concluding remarks and outlines future directions, particularly for scaling up Zn-Cu cells for niche applications and enhancing their educational utility through data-driven design tools.

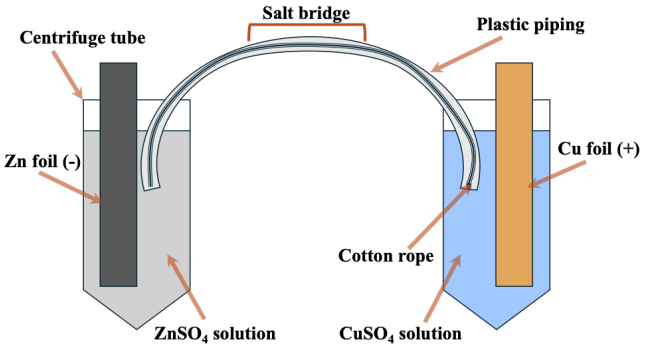

Figure 1. *Zn-Cu galvanic half-cell schematic.*

2. Methodology

2.1 Experimental design

This study investigated the influence of electrolyte concentration on the performance of zinc–copper galvanic cells. Each cell was constructed using Zn and Cu electrodes immersed in $ZnSO_4$ and $CuSO_4$ solutions, respectively. Electrolyte concentrations were systematically varied from 0.5 M to 2.0 M to assess their effect on open-circuit voltage (V_{oc}), short-circuit current (I_{sc}), and the cell's capacity to power LEDs. Measurements were recorded under both open-circuit and short-circuit conditions. Cells were tested as single units and in series and parallel configurations. LEDs with varying forward voltage thresholds were used to evaluate practical power output, P_{dc} (1). The materials and equipment used in this experiment are listed in Table 1.

$$P_{dc} = V_{dc} \times I_{dc}, \text{ [W]} \quad (1)$$

where V_{dc} I_{dc} – dc voltage and current of the battery (connected galvanic cells).

$$E_j = P_{dc} \times t, \text{ [J]} \quad (2)$$

E_j is the energy output, determned as a product of power P_{dc} and time t in seconds. Similarly, the specific energy per volume:

$$E_{js} = \frac{E_j}{Vol}, \text{ [J]} \quad (3)$$

where $E_j -$ energy output and $Vol -$ is the volume of the electrolyte.

Table 1
List of materials used in the investigation.

Equipment	Quantity	Parameter
Zn foil strips[1]	3	6 cm
Cu foil strips[2]	3	6 cm
Aqueous $ZnSO_4$ solution[3]	60 mL	2.0 mol/L
Aqueous $CuSO_4$ solution[4]	60 mL	2.0 mol/L
Aqueous KCl solution[5]	5	2.0 mol/L
Deionised water	120 mL	
Cotton ropes	3	≈20 cm
U-shaped plastic pipe lengths	3	≈20 cm
Centrifuge tubes	6x 50 mL	
Dual-ended wired alligator clips	4	
Digital multimeter	1	
LED lights in colours green, blue, white, yellow, red	6	
Beaker	100 mL	
Measuring cylinder	100 mL	
Plastic pipettes	2	
Test tube rack	1	
Electronic stopwatch	1	

2.2 Cell Assembly

The necessary equipment was gathered, and 3 lengths of cotton rope were submerged in a beaker containing 50 mL of 2.0 mol/L aqueous KCl solution. The 100 mL measuring cylinder and a plastic pipette were used to create 3 centrifuge tubes of varying concentrations for each electrolyte according to the volumes listed in Table 2.

Table 2
Required volumes for electrolyte solutions of varying concentrations.

Electrolyte Concentration (mol/L)	Volume of electrolyte solution required (mL)	Volume of deionised water required (mL)
0.5	10	30
1	20	20
1.5	30	10

[1] Zinc Sheet (Chem Supply – TG 0.1 mm thick) [ZT006-500G]
[2] Copper metal foil (Chem Supply – LR 0.1 mm thick) [CL054-500G]
[3] Zinc sulfate heptahydrate (Chem Supply - AR grade) ZA012-500G
[4] Copper (II) sulphate pentahydrate (Univar, AR, AJA171-500G)
[5] Potassium chloride (Univar, AR, AJA383-500G)

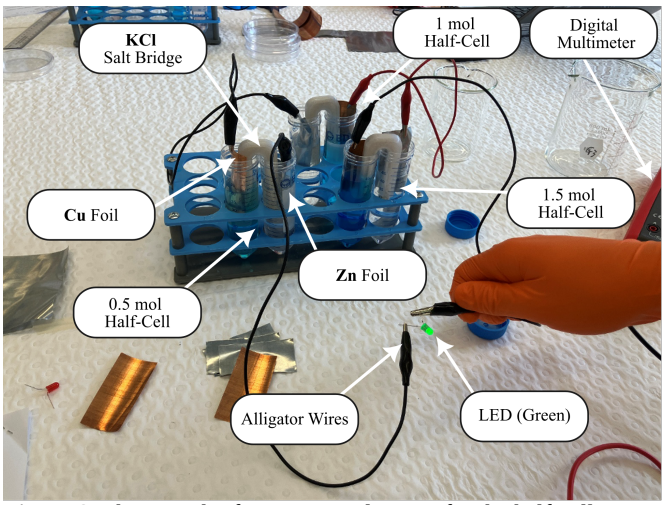

Figure 2. Photograph of experimental set-up for the half-cell series, seen with 3 half-cells illuminating the green LED.

The 3 saturated lengths of cotton rope were removed from the KCl solution and threaded through the 3 lengths of U-shaped plastic piping, to create 3 salt bridges for the half-cells. The 6 centrifuge tubes were arranged in pairs in the test tube rack, with a centrifuge tube containing $ZnSO_4$ solution placed adjacent to the centrifuge tube containing $CuSO_4$ solution of the same concentration. The centrifuge tube pairs, Zn foils, Cu foils, and salt bridges were set up creating 3 galvanic half-cells with electrolyte concentrations of 0.5, 1, and 1.5 mol/L. The foils were submerged ≈ 1/3 of the way into the electrolyte solution, mirroring the setup outlined in Figure 1.

2.3 Measurement protocol

The electronic multimeter was used to measure the voltage and current of each half-cell using two alligator clips which connected the positive terminal of the multimeter to the Cu foil and the negative terminal of the multimeter to the Zn foil. The results were recorded.

For each half-cell the free ends of the alligator clips were clipped onto the metal legs of the red LED to test whether the half-cell was able to light up the LED. If the LED did light up, it was allowed to glow for 3 seconds, measured with the stopwatch. Observations were recorded. (Note: other LED colours were not tested as they required higher voltages and currents than the red LED).

The following half-cell series were assembled by connecting the Zn foil of one to the Cu foil of the next using alligator wires; 0.5 and 1 mol concentrations, 1 and 1.5 mol concentrations, and 0.5, 1, and 1.5 concentrations. The process of voltage and current measurement was repeated for each configuration, and the results were recorded. The red, white, yellow, blue, and green LEDs were tested for each configuration using the same method as outlined above, and the results and observations were recorded.

3. Results

3.1 Analysis of galvanic cell performance: Influence of electrolyte concentration and cell configuration.

The results clearly demonstrate how both electrolyte concentration and cell configuration influence the output of Zn-Cu galvanic cells, as presented in Table 2. According to electrochemical theory, especially the Nernst equation (4), increasing the concentration of ions in solution increases the electrode potential.

This was evident in the data: although all single-cell setups showed similar theoretical voltages (~1.1 V), those with higher molarity showed slightly higher measured voltages and current-as you can see in Figure 4.

$$E_e = E^\circ - \frac{RT}{nF}\ln Q, \quad (4)$$

where $E^\circ -$ is standing electrode potential, $R -$ universal gas constant, $T -$ temperature (K), $n -$ number of electrons transferred, $F -$ Faraday's constant, and $Q -$is the reaction quotient.

Table 3
Raw voltage, current, and LED data for each half-cell configuration.

Half-Cell Configuration	Theoretical Voltage, (V)	Voltage, (V)	Current, (mA)	LED Light Illumination Observed				
				Red	Yellow	White	Blue	Green
Single half-cell, (0.5 mol/L concentration)	1.101[1]	1.075	1.43	X	X	X	X	X
Single half -cell, (1 mol/L concentration)		1.076	1.411	X	X	X	X	X
Single half-cell, (1.5 mol/L concentration)		1.077	1.315	X	X	X	X	X
2 half-cells in series, (0.5 and 1 mol/L concentrations)	2.2	2.075	1.117	✓	X	X	X	X
2 half-cells in series, (1 and 1.5 mol/L concentrations)		2.145	1.538	✓	X	X	X	X
3 half-cells in series, (0.5, 1, and 1.5 mol/L concentrations)	3.3	3.188	1.671	✓	✓	✓	✓	✓

Table 4
Calculated output and specific power and energy for each half-cell configuration.

Half-Cell Configuration	Electrolyte Volume, (mL)	Submerged Electrode Area, (cm2)	LED illumination time, (s)	Power Output, (mW)	Specific Power, (mW/cm^2)	Energy Output, (mJ)	Specific Energy (mJ/mL)
Single half-cell, (0.5 mol/L concentration)	40	6	-	1.538	0.256	-	-
Single half -cell, (1 mol/L concentration)			-	1.519	0.253	-	-
Single half-cell (1.5 mol/L concentration)			-	1.417	0.236	-	-
2 half-cells in series (0.5 and 1 mol/L concentrations)			3	2.318	0.386	6.954	0.174
2 half-cells in series (1 and 1.5 mol/L concentrations)				3.3	0.55	9.9	0.248
3 half-cells in series (0.5, 1, and 1.5 mol/L concentrations)				5.327	0.889	15.981	0.4

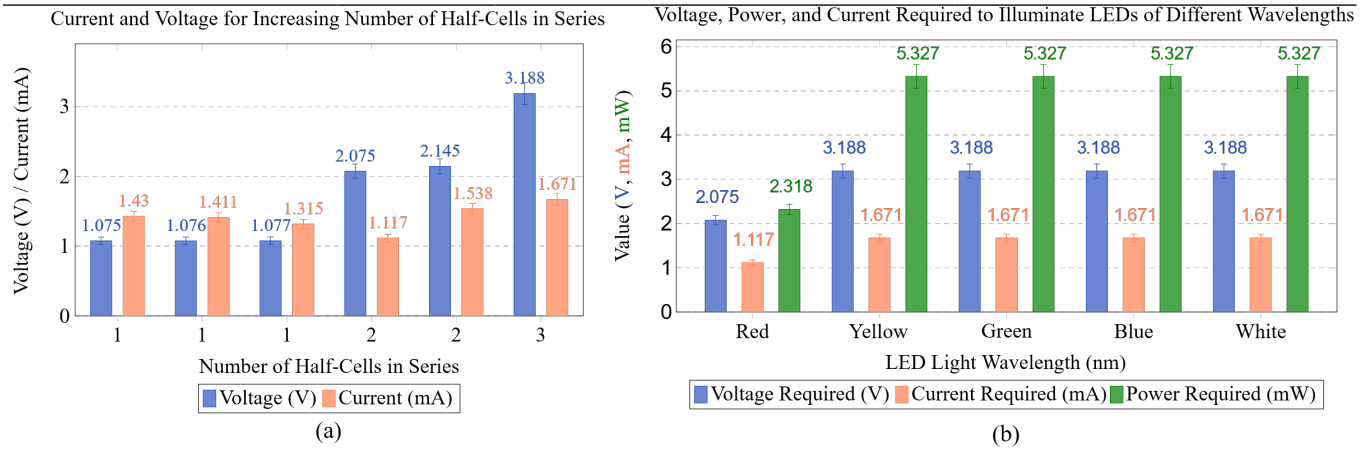

Figure 3. Experimental results: electrical parameters of series connected half-cells. (a) Voltage and current by cell configuration, (b) comparison of LED voltage thresholds to switch on the LED and half-cell dc power output.

None of the single cells produced enough power to illuminate any LEDs. In contrast, two cells in series powered the red LED, and three cells powered all LEDs, refer to Table 2 and Figure 3(b). This confirmed the theoretical prediction that series connections increase total voltage of the connected half-cells, whilst keeping the same dc current flow, albeit with some variations due to the cable resistance change and imperfect connection of alligator wires, as shown in Figure 3(a). Furthermore, the linear relationship with the increasing number of half-cells (i.e. total series dc voltage) and total power delivered to LED can be observed Table 3. From chemical perspective, higher electrolyte concentration and series configurations yielded higher energy output, so that various half-cells configurations and connection can results in different voltage-current output from the resultant battery system.

During the work only one measurement per LED was performed, hence the error bars are established using an assumed fixed uncertainty, rather than a statistical deviation. In this work, 5% deviation was utilised to estimate the possible measurements errors and error bars in Figure 3, as per (5). Instead, the error bars were created using an assumed percentage uncertainty, specifically:

$$\Delta X_i = 0.05 \times x_i, \quad (5)$$

where x_i – is the measurement (i.e. voltage and current).

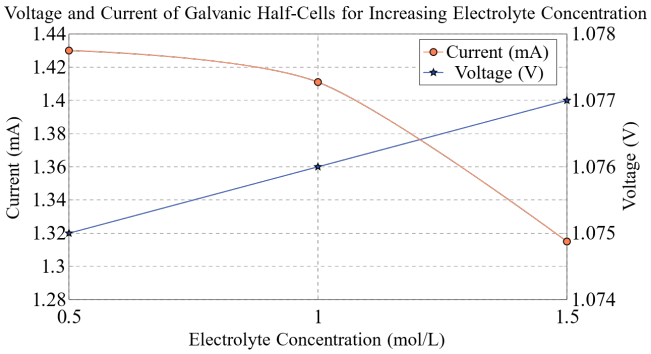

Figure 4. Voltage and current across different electrolyte concentrations.

4. Discussion

4.1 Relationship between results and theory of voltage

This investigation into Zn-Cu galvanic cells provides valuable insights into electrochemical principles, with the experimental results mostly aligning with theoretical expectations derived from these principles. In particular, standard reduction potentials (SRP), which show that the theoretical voltage for a Zn-Cu galvanic cell under standard conditions should approximately be 1.10 V, calculated from the difference in SRPs of Zn and Cu. The SRP value for the Zn^{2+}/Zn cell is -0.76 V, while the SRP value for the Cu^{2+}/Cu cell is +0.34 V. Since the Zn is being oxidised, the SRP is subtracted, thus the theoretical cell voltage $E°$ = (+0.34) – (– 0.76) = 1.10 V [10], as represented in Table 2.

This theoretical value for voltage was closely represented by the measured voltages for the single cell configurations, which ranged from 1.075 V to 1.077 V depending on the concentration of the electrolyte solutions. The measured V_{oc} had a deviation of less than 2.3% when compared to the theoretical value, reflecting that the experimental setup closely approximated standard reaction conditions

The minimal increase in the voltage as the concentration of the electrolyte increased may be attributed to the Nernst equation, which predicts that increasing ion concentration at the cathode and decreasing ion concentration at the anode will increase the cell potential at non-standard conditions, where a lower value for the reaction quotient Q would result in a larger overall cell potential E [11]. However, while the concentrations of the anode and cathode were increased during the experiment, the concentration of the anode was always the same as the cathode for each trial. Thus, it is likely that the slight increase in voltage across the single half-cells was not due to the effect of the Nernst equation.

The explanation for the increase in voltage could be attributed to increase in the absolute (instead of the relative) concentrations of the Zn^{2+} and Cu^{2+} ions, which enhanced the measured performance of the galvanic cell through the voltage. This is due to real-world electrochemical effects, such as the higher ion concentration improving the availability of ions at the electrode surfaces, which means that there are more ions that can be used up in the redox reaction [12]. This allows the redox reaction to proceed at a faster rate than at a lower concentration, allowing the cell to maintain a higher voltage, especially under load such as when powering the LED light. A greater number of ions in the electrolyte solution also increases the electrolyte's ionic conductivity, which could reduce the internal resistance and help to minimise the voltage lost across the cell, which maximises the voltage output [13]. However, these effects were likely minimal because the electrolyte solutions were already fairly saturated at all concentrations, hence the relatively low (but measurable) increase in the voltage produced by the cell.

From an engineering perspective, the experimental results demonstrate that increasing electrolyte concentration slightly improves the measured voltage output of the Zn-Cu galvanic cells. While the theoretical voltage based on the Nernst equation should remain constant because the electrolyte concentrations of Zn^{2+} and Cu^{2+} remained equal to one another, the observed increase in voltage at higher concentrations is not due to changes in the potential predicted by the Nernst equation [14] Instead, this reflects real-world improvements in the performance of the electrochemical system; higher ion concentrations enhance ionic conductivity, increase ionic availability for redox reactions and help slightly improve the voltage output. However, even with these improvements, the single half-cells were still unable to produce enough voltage required to power the LED lights, demonstrating the real-world engineering limitations of the galvanic single half-cell design.

4.2 Effect of electrolyte concentration on current

The decrease in current due to the increase in concentration can be attributed to the different physical and chemical reactions that take place due to this oversaturation. These potential changes are likely due to the formation of a thick layer of solid electrolytes over the metal sheets. According to Ohm's law, voltage (V) is equal to current (I) multiplied by resistance(R), as per (6).

$$V = IR. \quad (6)$$

Although increasing the electrolyte concentration generally improves ionic conductivity and reduces internal resistance, a marginal decrease in current was observed at the highest concentration. This may be attributed to non-ideal factors such as increased solution viscosity or concentration polarisation near the electrode surfaces, which can hinder ion mobility. However, within the tested concentration range, these effects are likely minimal, and the slight drop in current could also result from measurement variability or inconsistencies in electrode surface

4.3 Effect of electrolyte concentration on power output

This trend also influenced the specific power and energy of the cells. Specific power, which reflects the rate of energy delivery per unit electrode area, decreased in single-cell setups as concentration increased—again due to reduced current. Specific energy, representing total energy output per unit volume of electrolyte, was not measurable for single cells as they could not power LEDs. This highlights the limitations of relying solely on concentration to enhance performance. While higher concentrations slightly improved voltage due to increased ionic conductivity and ion availability, the overall energy delivery capacity remained limited without further system enhancements.

4.4 Effects of Series Connection on Voltage and LED Activation

According to Kirchhoff's law, the total voltage across the series of cells is determined by the sum of the individual cell voltages [15]. Thus, as each cell produces 1.10 V, two cells in series should produce 2.20 V and three cells in series should theoretically produce 3.30 V. Whilst the individual voltage of a single cell (1.10 V) was insufficient to power any of the LEDs, connecting the cells in series increased the combined voltage, which allowed the system to reach higher voltage thresholds required to power the LEDs [14] This is shown by Table 3, which demonstrates that two half-cells in series produced voltages of 2.075 V and 2.145 V; this voltage was high enough to power the red LED light, which required a voltage of 2.075 V. However, this was not sufficient to power the other cells, and as such three cells were connected in series, obtaining a voltage of 3.188 V, as seen in Table 3. This allowed the system to successfully power all the LEDs of each colour in decreasing order of voltage from green to red.

To ensure consistent and reliable testing, LEDs were evaluated in decreasing order of their minimum voltage threshold, beginning with the green LED and ending with the red. This approach was selected in order to minimise the risk of current depletion or voltage drop due to the gradual loss of available energy as the galvanic cell is used up over time [16]. Since the higher voltage LEDs (such as green) require greater amounts of energy to light up, testing them first ensured that the system of cells was operating at its maximum available voltage and current output. If the lower voltage LEDs (such as red) had been tested first, the system of cells would have likely experienced a measurable decline in performance due to a depletion of ions or other factors causing a loss in the available energy from the cells, potentially inhibiting the successful light-up of the later LEDs, which have higher voltage thresholds and greater energy requirements. By testing the LEDs from the highest to lowest voltage threshold, the experimental design ensured that the system was able to power the lights with its full energy capacity, without prematurely exhausting its energy potential.

4.5 Analysis of specific power and specific energy

The specific power, measured in mW/cm^2 (although usually measured in power per unit mass) demonstrates how quickly a system can deliver energy to an output, per unit area of the electrode surface [17]. This indicates the rate at which energy can be delivered, as a higher specific power corresponds to more efficient uses of the electrode surface for fast and effective energy delivery to the power output. This can be seen by the higher specific power values in Table 4 for the cells in series, however the specific power decreases as concentration increases for the single half-cells, due to the decrease in the current.

The specific energy, measured in mJ/mL, represents the total amount of energy delivered per unit volume of electrolyte solution. It corresponds to the system's ability to store and release energy over time, rather than the rate of delivery [18]. As seen in Table 4, there were no energy values determined for the single half-cells, as these cells were unable to power any of the LED lights individually, and thus there was no measurable energy that was delivered to a load. The highest specific energy was observed in the configuration with three half-cells in series, reaching 0.4 mJ/mL, indicating that combining cells not only increases voltage but also enhances the total energy output. Interestingly, while higher electrolyte concentrations generally improve voltage and current, the specific energy did not increase linearly with concentration. This suggests that beyond a certain point, factors such as internal resistance or ion saturation may limit the efficiency of energy transfer for the system of cells.

The specific energy values were calculated per unit volume of electrolyte; the specific power values were calculated per unit area of the submerged electrode. However, this likely led to inaccuracies with the true value of the specific power, because the area of the submerged electrode was assumed to be 6 m^2 for all the half-cells, leading to inconsistencies that were not considered. This had less effect in the specific energy, as the electrolyte volume was measured using a measuring cylinder, which is much more accurate than a human submerging the electrodes to approximately the same level for each cell. Thus, estimating the electrode submersion depth caused more variability for the surface area calculations and limited the accuracy of the specific power calculations.

4.6 Limitations and future improvements

Despite the overall success of the experimental setup, several limitations may have influenced the accuracy and reliability of the results. One key limitation is electrode fouling, where the accumulation of reaction by-products or solid electrolyte layers on the electrode surfaces can hinder electron transfer and reduce current output [19]. This is particularly relevant at higher electrolyte concentrations, where oversaturation may accelerate such deposition. Another issue is ionic depletion, especially during prolonged operation or repeated testing. As ions are consumed in redox reactions, their local concentration near the electrode surfaces can drop, leading to reduced reaction rates and voltage instability. Additionally, measurement error may have occurred due to inconsistencies in electrode submersion depth [20] manual handling of components, and contact resistance in the alligator clips and wiring. To address these limitations, future experiments could incorporate standardised electrode holders to ensure consistent surface area exposure and stirring systems (or possible flow systems with an electrolyte reservoir) to maintain uniform ion distribution and prevent depletion [21]. Repeating measurements and using statistical analysis would also improve data reliability. Finally, upgrading to low-resistance connectors and more precise instrumentation would help minimise electrical losses and improve the accuracy of voltage and current readings.

4.7 Evaluation of engineering applications

The findings of this investigation have direct applications to real world engineering problems, particularly in areas such as energy efficiency, sustainability and cost effectiveness. Practically, in the design of batteries for devices such as medical implants and portable electronics, it is important to optimise specific power and specific energy in order to deliver reliable performance without excessive inputs of materials or energy. This is particularly important in medical implantable devices such as pacemakers, which need to be small, safe and effective [22]-[23]. Furthermore, in the field of sustainable batteries, electrochemical cells have been used to create rechargeable batteries [24]. While increasing the concentration of electrolytes and linking cells in series improved the voltage, power and energy outputs, this approach is likely not scalable to more intricate and larger

batteries due to the higher cost, environmental impact of high-concentrated solutions and the configurational complexities of cells in series on a large scale. Also, there are likely to be diminishing returns of voltage and power output at higher concentrations, due to the effects of reduced current from increased internal resistance. This demonstrates the importance of understanding the real-world engineering limitations when trying to optimise electrochemical enhancements to the system. This highlights the need for a system design that considers sustainability of materials, manufacturability, longevity of the system, and the reality of real-world conditions in addition to electrochemical performance [25]. These insights can be informed by considerations such as the Nernst equation. However, even considerations such as these are somewhat theoretical, and cannot fully account for discrepancies in real-world systems.

5. Conclusion

The study demonstrated the significant impact of electrolyte concentration and cell configuration on the performance of Zn-Cu galvanic cells. Connecting three half-cells in series yielded the highest performance, achieving 3.19 V, 1.67 mA, and 15.98 mJ of energy output (refer to Table 2 and Table 3). In contrast, individual cells (~1.1V) were unable to power even the lowest-threshold LED, underscoring the importance of voltage summation in series connections.

These findings illustrate the importance of both chemical environment and system arrangement in optimising electrochemical performance. Significant trade-offs existed between simplicity of setup and the voltage required to power more highly demanding electronic components. While elevated electrolyte concentrations improve performance, practical applications must balance this with considerations such as cost, stability, and environmental safety of concentrated solutions.

A valuable direction for future research would be to investigate the effects of alternative electrolyte compositions, such as biodegradable or polymer-based solutions, which may enhance sustainability while maintaining sufficient ion conductivity and redox activity over repeated cycles.

Authorship

The outlined investigation was conducted and performed by all authors. Anastasiia Danshyna completed all formatting for data visualisation tables (Tables 1-3) and figures (Figures 1-5), contributed to results section 3.1, wrote the conclusion, and carried out the full formatting and structuring of the article. Grace Mihaljevic completed the methods and equipment sections, and contributed to Tables 1-3, and Figures 1-5. Stefano Furlan completed the discussion section (4.1, 4.3 -4.7), interpreting results through electrochemical engineering principles. Isaac Sleath completed the abstract and introduction sections. Alexander Palmer completed the discussion section (4.2), interpreting the effects of oversaturation on galvanic cells and the connection of batteries in a series in relation to Kirchhoff's law. Tutors (Masoomeh Asghar Nejad-Laskoukalayeh, Jordan Kambanis and Benedict Tai,) provided task direction and project assistance, Dr Thomas Whittle designed the experiment, Dr David Alam facilitated project resources and guidance on conceptual direction, and Dr. Gobinath Rajarathnam ideated conceptual direction, research and writing guiding frameworks, and direct project supervision.

Acknowledgements

The authors acknowledge the limited use of generative artificial intelligence (ChatGPT) to support the writing of this article. However, all the report's content was developed independently by the authors.

References

[1] G. Li *et al.*, "Developing Cathode Materials for Aqueous Zinc Ion Batteries: Challenges and Practical Prospects," *Advanced Functional Materials*, vol. 34, no. 5. 2024. doi: 10.1002/adfm.202301291.

[2] M. Al-Amin, S. Islam, S. U. A. Shibly, and S. Iffat, "Comparative Review on the Aqueous Zinc-Ion Batteries (AZIBs) and Flexible Zinc-Ion Batteries (FZIBs)," *Nanomaterials*, vol. 12, no. 22. 2022. doi: 10.3390/nano12223997.

[3] B. Tang, L. Shan, S. Liang, and J. Zhou, "Issues and opportunities facing aqueous zinc-ion batteries," *Energy and Environmental Science*, vol. 12, no. 11. 2019. doi: 10.1039/c9ee02526j.

[4] Z. Salameh, *Renewable Energy System Design*. 2014. doi: 10.1016/C2009-0-20257-1.

[5] Battery lab instructions. Preparation and Testing of Galvanic Cells Using Copper and Zinc Electrodes. 2025. *USYD CBE Materials.*

[6] H. Zhang *et al.*, "Using Li+ as the electrochemical messenger to fabricate an aqueous rechargeable Zn-Cu battery," *Chemical Communications*, vol. 51, no. 34, 2015, doi: 10.1039/c5cc00575b.

[7] A. Jameson, A. Khazaeli, and D. P. J. Barz, "A rechargeable zinc copper battery using a selective cation exchange membrane," *Journal of Power Sources*, vol. 453, 2020, doi: 10.1016/j.jpowsour.2020.227873.

[8] G. P. Rajarathnam and A. M. Vassallo, "The Zinc/Bromine Flow Battery," *SpringerBriefs in Energy*, 2016.

[9] Feiner, A. S., & McEvoy, A. J. (1994). The nernst equation. *Journal of chemical education*, 71(6), 493.

[10] C. Shin, L. Yao, S. Y. Jeong, and T. N. Ng, "Zinc-copper dual-ion electrolytes to suppress dendritic growth and increase anode utilization in zinc ion capacitors," *Sci. Adv.*, vol. 10, no. 1, Art. no. eadf9951, Jan. 2024, doi: 10.1126/sciadv.adf9951.

[11] L. Wen et al., "Effect of composite conductive agent on internal resistance and performance of lithium iron phosphate batteries," *Ionics*, vol. 28, no. 7, pp. 3145–3153, 2022.

[12] Y. S. Hu, Y. Lu, "The Mystery of Electrolyte Concentration, from Superhigh to Ultralow," *ACS Energy Lett*, vol. 5, no. 11, pp. 3633-3636, 2020 https://pubs.acs.org/doi/full/10.1021/acsenergylett.0c02234 (12)

[13] L. Liu, J. Zhu, and L. Zheng, "An effective method for estimating state of charge of lithium-ion batteries based on an electrochemical model and Nernst equation," *IEEE Access*, vol. 8, pp. 211738–211749, 2020.

[14] R. Drummond, L. D. Couto, and D. Zhang, "Resolving Kirchhoff's laws for parallel li-ion battery pack state-

estimators," *IEEE Trans. Control Syst. Technol.*, vol. 30, no. 5, pp. 2220–2227, 2021.

[15] K. Lacina, J. Sopoušek, P. Skládal, and P. Vanýsek, "Boosting of the output voltage of a galvanic cell," *Electrochimica Acta*, vol. 282, pp. 331–335, 2018.

[16] L. Redley, "Lithium batteries for pulse power," presented at the 10th Annual Battery Conf. on Applications and Advances, Long Beach, CA, USA, 1990. [Online]. Available: https://www.osti.gov/servlets/purl/6118809-p2HtVA/

[17] P. M. Biesheuvel, M. van Soestbergen, M. Z. Bazant, "Imposed currents in galvanic cells," *Electrochimica Acta*, vol. 54, no. 21, pp. 4857-4871, 2009. https://doi.org/10.1016/j.electacta.2009.03.073

[18] R. V. Kumar and T. Sarakonsri, *Introduction to Electrochemical Cells*, in *Rechargeable Ion Batteries*, Singapore: Springer, 2022.

[19] B. L. Hassen, S. Siraj, D. K. Y. Wong, "Recent strategies to minimise fouling in electrochemical detection systems," *Reviews in Analytical Chemistry*, vol. 35, no. 1, 2016. https://www.degruyterbrill.com/document/doi/10.1515/revac-2015-0008/html#APA

[20] P. Vanýsek, "Impact of electrode geometry, depth of immersion, and size on impedance measurements," *Canadian Journal of Chemistry*. 1997, https://doi.org/10.1139/v97-194.

[21] Gunawan *et al.* "Energy storage system from galvanic cell using electrolyte drom a plant as an alternative renewable energy," *IOP Conf. Series: Material Science and Engineering*, 2019, doi:10.1088/1757-899X/509/1/012045.

[22] D. C. Bock, A. C. Marschilok, K. J. Takeuchi, and E. S. Takeuchi, "Batteries used to power implantable biomedical devices," *Electrochimica Acta*, vol. 84, pp. 155–164, 2012, doi: 10.1016/j.electacta.2012.03.057.

[23] R. Latham, R. Linford, W. Schlindwein, "Biomedical applications of batteries," *Solid State Ionics*, vol. 172, no. 1-4, pp. 7-11, 2004 https://doi.org/10.1016/j.ssi.2004.04.024.

[24] S. Mypati, A. Khazaeli, D. P. J. Barz, "A novel rechargeable zinc-copper battery without a separator," *Journal of Energy Storage*, vol 42, 2021, https://doi.org/10.1016/j.est.2021.103109

[25] L. B. Wheeler, B. A. Whitworth, A. L. Gonczi, "Engineering design challenge: building a voltaic cell in the high school chemistry classroom," *The Science Teacher*, vol. 81, no. 9, pp. 30-36, 2014, https://doi.org/10.2505/4/tst14_081_09_30

